

CONSENSUS TREE ESTIMATION WITH FALSE DISCOVERY RATE CONTROL VIA PARTIALLY ORDERED SETS

MARIA A VALDEZ CABRERA ¹, AMY D WILLIS ¹, AND ARMEEN TAEB ²

ABSTRACT. Connected acyclic graphs (trees) are data objects that hierarchically organize categories. Collections of trees arise in a diverse variety of fields, including evolutionary biology, public health, machine learning, social sciences and anatomy. Summarizing a collection of trees by a single representative is challenging, in part due to the dimension of both the sample and parameter space. We frame consensus tree estimation as a structured feature-selection problem, where leaves and edges are the features. We introduce a partial order on leaf-labeled trees, use it to define true and false discoveries for a candidate summary tree, and develop an estimation algorithm that controls the false discovery rate at a nominal level for a broad class of non-parametric generative models. Furthermore, using the partial order structure, we assess the stability of each feature in a selected tree. Importantly, our method accommodates unequal leaf sets and non-binary trees, allowing the estimator to reflect uncertainty by collapsing poorly supported structure instead of forcing full resolution. We apply the method to study the archaeal origin of eukaryotic cells and to quantify uncertainty in deep branching orders. While consensus tree construction has historically been viewed as an estimation task, reframing it as feature selection over a partially ordered set allows us to obtain the first estimator with finite-sample and model-free guarantees. More generally, our approach provides a foundation for integrating tools from multiple testing into tree estimation.

1. INTRODUCTION

Connected acyclic graphs, or *trees*, represent hierarchical organizations of categories and arise in many fields in the natural, medical and social sciences. For example, trees can represent the shared ancestry of organisms (Darwin 1859, Felsenstein 2004); the development and diversification of languages (Gray & Atkinson 2003); infection transmission across a population (Haydon et al. 2003); and physical branching structures in the lungs, arteries and brain (Bendich et al. 2016). Trees also can be used to represent decision-making algorithms, including flowcharts for human resources management, programs in computer science, and to represent predictive models in statistical learning. In many applications, there does not exist a single tree (Wang & Marron 2007). For example, different genes may follow distinct evolutionary histories (Pamilo & Nei 1988, Maddison 1997); different models may be predicted using different datasets (Breiman 2001); and elements of distinct languages may diversify in different orders (Nakhleh et al. 2005). Analyzing collections of trees presents challenges that do not arise in vector-valued data settings. The number of possible trees is super-exponential in the number of leaves, and therefore it is common that no tree is observed more than once in a sample. Measures of central tendency such as means and medians are non-trivial to define, let alone compute. Dimensionality and data summarization challenges are further exacerbated when the observed trees have non-identical leaf labels and non-binary branching.

1.1. Our contributions. In this paper, we develop and study a method for estimating a summary tree (or *consensus tree*) using a tree-valued sample. A key innovation is recasting a statistical problem that has historically been viewed as an estimation problem as a model selection problem, which allows us to provide finite-sample guarantees on the estimator for an extremely broad class of generative models. Specifically, we propose that edges and leaves on trees should be interpreted as features. In contrast to typical feature selection problems, features on trees are highly structured: edges can only partition leaves that are present; and not all edges are mutually compatible. To address this, we define a *partially ordered set* (poset) over the set of all possible binary and non-binary trees on a maximal leaf set, and use it to enforce leaf-presence and edge-compatibility constraints. We use the poset structure to define the number of true discoveries and

¹ DEPARTMENT OF BIostatISTICS, UNIVERSITY OF WASHINGTON

¹ DEPARTMENT OF BIostatISTICS, UNIVERSITY OF WASHINGTON

² DEPARTMENT OF STATISTICS, UNIVERSITY OF WASHINGTON

E-mail addresses: mariavc@uw.edu, adwillis@uw.edu, ataeb@uw.edu.

false discoveries of a tree-valued estimate with respect to a tree-valued parameter, and present a consensus tree estimation method that controls the false discovery rate (FDR). Features on the resulting estimates can be assigned interpretable stability scores, reflecting the support for the feature by the trees in the sample. Intuitively, edges that are not well-supported in the sample do not appear in the consensus estimate, and similarly for leaves whose placement is uncertain. Our work also has applications in uncertainty quantification for trees more generally, as stability scores can be applied to assess the evidence in sample trees for any tree estimate, not just in our proposed approach.

Aside from offering the first consensus tree estimator with formal FDR guarantees, our method also accommodates collections of trees that do not share the same leaf set. This is a major practical impediment to many existing approaches to consensus tree estimation, as surveyed in more detail below. While our method can be applied to any collection of leaf-labeled unweighted trees, our proposal was initially motivated by analyzing collections of phylogenetic trees of ancient genes. As simple organisms evolved to give rise to complex organisms, new genes emerged and early genes were lost. As a result, few genes are universally present across diverse organisms. Our feature selection approach naturally accommodates trees with missing leaves, and we therefore demonstrate our approach by integrating the conflicting information provided by distinct ancient genes to evaluate the strength of evidence for estimating the branching order of early life. We consider interpretable uncertainty measures crucial to accurately communicating evidence for the order of divergence events that occurred more than 2 billion years ago (Betts et al. 2018), and our method’s stability scores are well-suited to this purpose. That said, because the guarantees on our estimator are model-agnostic, our approach is applicable beyond phylogenetic applications.

1.2. Related work. Since our work brings together tree estimation and model selection, we review related work from both areas.

Tree estimation and uncertainty. Many approaches to estimating a single hierarchical structure from tree-valued data exist. When all trees in the dataset share a leaf set, split thresholding provides a simple way to integrate the dataset by retaining edges (splits) present in at least $100 \times p\%$ of the trees. The case $p = 0.5$ is *majority rule* and $p = 1$ is *strict consensus* (Adams 1972, Margush & McMorris 1981). Another conceptually simple approach is a Fréchet mean or median, which minimizes the distance to the trees in the sample with respect to a specified distance metric on trees (Robinson & Foulds 1981, Barthélemy & McMorris 1986, Miller et al. 2015) and over a specified parameter space. Like split thresholding, this approach typically assumes a common leaf set so that distances are well-defined. More complex approaches include data-aggregation pipelines that bypass individual tree construction (e.g., concatenation-based workflows in phylogenetics) (Wu & Eisen 2008, Segata et al. 2013, Lee 2019, Asnicar et al. 2020); methods that maximize agreement over small induced substructures (Mirarab et al. 2014, Zhang et al. 2018, Sayyari & Mirarab 2016, Avni & Snir 2018, 2019); model-based approaches (Galtier 2007, Liu et al. 2010, Szöllösi et al. 2013, Chernomor et al. 2016); concordance-based frameworks (Larget et al. 2010); and distance-based methods (Saitou & Nei 1987, Felsenstein 1997).

Among the myriad approaches, methods that maximize agreement over substructures have been widely adopted. The most popular methods within this class find the tree that maximizes the number of quartets (four-leaf induced topologies) represented in the sample. Unlike split thresholding, this approach can accommodate unequal leaf sets, and the consistency of the quartet trees for a summary of the data distribution has been shown under a number of parametric models (Mirarab et al. 2014, Yan et al. 2022, Markin & Eulenstein 2021, Legried et al. 2021). However, consistency is an asymptotic property and does not quantify finite-sample uncertainty. To our knowledge, general finite-sample guarantees of accuracy are not available for either quartet-maximization or split-thresholding estimators. In principle, the approach given in (Degnan et al. 2009, Appendix 8) can be used to determine the sample size needed to attain a target probability of recovering the underlying tree, but this requires knowledge of the underlying data distribution and hence knowledge of the target of estimation, thus limiting its utility in practice. An additional consideration in consensus tree estimation is the support of the parameter space. Popular algorithms for quartet maximization estimate binary trees (Mirarab et al. 2014, Zhang et al. 2018), while split thresholding does not force estimates to be binary. Our perspective is that estimates should be binary only when justified by the dataset, with ambiguous splits left unresolved.

Multiple testing and model selection. For many models, it is straightforward to connect model selection to hypothesis testing; e.g. in regression, the inclusion of a variable corresponds directly to a rejection of a hypothesis. In more complicated models such as trees, however, it is difficult to relate model selection to a collection of hypotheses. In trees, for example, an edge cannot be considered in isolation; its inclusion or exclusion affects the other possible edges. There are methods for hierarchical hypothesis testing, where if one hypothesis is not rejected, this impacts other hypotheses, e.g. G’Sell et al. (2013), Li & Barber (2015), Ramdas et al. (2019), Yekutieli (2008), Lynch et al. (2016). However, for trees, it is not even clear how to construct such a hierarchy. Our poset framework provides a formulation for a hierarchy of hypothesis tests, and opens the door for developing false discovery controlling procedures for tree selection. As described in Section 5.2, even after formalizing hypothesis tests using posets, existing methods are not suitable for FDR control, and thus a new procedure is developed in this paper.

Statistical model selection over posets was first proposed in Taeb et al. (2024). For a given model selection problem, they organize associated models in a poset and present a framework to measure and control false discoveries. Our work builds on top of Taeb et al. (2024) in several substantive ways. In particular, Taeb et al. (2024) do not identify a poset underlying trees, and they do not provide a procedure to control the FDR.

2. BACKGROUND

2.1. Tree preliminaries. Throughout this section, let X be a fixed, finite set of labels. The labels will typically denote categories, such as species in phylogenetics, viral strains in infectious disease modeling, and languages in linguistics.

Unrooted tree. Throughout this paper, we take a tree $T = (V, E)$ over leaves X to be an undirected, connected, acyclic graph. The structure contains two feature types. The first feature type is its leaves (nodes of degree 1) are the set X . The second type is its edge set; we will use the notation $E(T)$ to denote the edge set of T .

Internal nodes. For an unrooted tree T over leaves X , its internal nodes are $V \setminus X$.

Split induced by an edge. Consider an unrooted tree $T = (V, E)$. Given an edge $e \in E$, removing e disconnects T into two components. Let $A \subset X$ and $B = X \setminus A$ be the set of leaf labels in each component. Then the edge e induces a split of X , denoted by $A|B$. We will denote the split associated with an edge e by S_e . A split $A|B$ is called *non-trivial* if both A and B contain at least two elements.

Internal edge. An edge $e \in E$ of an unrooted tree $T = (V, E)$ is an internal edge if it induces a non-trivial split.

Split set. A split set of an unrooted tree $T = (V, E)$, denoted $\mathcal{S}(T)$, is the set of all non-trivial splits induced by the edges of T . Formally, $\mathcal{S}(T) := \{A|B : \text{edge } e \in E \text{ induces a non-trivial split } A|B\}$. The set $\mathcal{S}(T)$ uniquely determines the topology of T up to isomorphism. Note that the cardinality of $\mathcal{S}(T)$ is equal to the number of internal edges.

Leaf set. The leaf set of tree $T = (V, E)$, denoted $\mathcal{L}(T)$, is the collection of its leaves X .

Resolved trees. An unrooted tree $T = (V, E)$ is completely unresolved if it has no internal edges, or equivalently, if $\mathcal{S}(T) = \emptyset$ (also known as a *star tree*). The tree T is fully resolved if every internal node has degree equal to three (also known as a *binary tree*). Note that the size of the split set is maximized for a fully resolved tree. The tree T is partially resolved if it is neither a star tree nor a binary tree.

Split compatibility. Given two splits $S_1 = A_1|B_1$ and $S_2 = A_2|B_2$ of the same leaf set $X = A_1 \cup B_1 = A_2 \cup B_2$, they are said to be compatible if both can be part of the same tree. This is equivalent to either $A_1 \subseteq A_2$, $A_1 \subseteq B_2$, $B_1 \subseteq A_2$ or $B_1 \subseteq B_2$.

Restriction of split set. Let $S = A|B$ be a non-trivial split of leaf set X , and let $Y \subseteq X$ be a subset of the leaves. The restriction of the split S to Y , denoted $\Phi_Y(S)$, is defined as $\Phi_Y(S) := (A \cap Y|B \cap Y)$ provided that both $A \cap Y$ and $B \cap Y$ both contain at least two leaves. If either side of the restricted split contains fewer than two leaves, the restriction $\Phi_Y(S)$ is considered undefined. Given a set of splits $\mathcal{S}(T)$ from a tree T with leaf set X , the restriction of the split set to $Y \subseteq X$, denoted $\Phi_Y(\mathcal{S}(T))$, is $\Phi_Y(\mathcal{S}(T)) := \{\Phi_Y(S) : S \in \mathcal{S}(T), \Phi_Y(S) \text{ is defined}\}$.

Restriction of tree. Let $A \subseteq X$ be a subset of the set of leaves in the tree $T = (V, E)$. We let $\Phi_A(T)$ denote the tree with leaf set A and split set $\Phi_A(\mathcal{S}(T))$.

Leaf removal. Given an unrooted tree $T = (V, E)$ that has leaf a , the tree $T_{\downarrow \text{leaf } a}$ is the tree after removing leaf a from T . Formally, the leaf set of $T_{\downarrow \text{leaf } a}$ is $\mathcal{L}(T) \setminus \{a\}$, and the split set of $T_{\downarrow \text{leaf } a}$ is $\{\Phi_{\mathcal{L}(T) \setminus \{a\}}(S) : S \in \mathcal{S}(T)\}$.

Collapsing edges. Given an unrooted tree $T = (V, E)$ with an internal edge $e \in E$, the tree $T_{\downarrow \text{edge } e}$ is the tree after collapsing the edge e in T . Formally, the leaf set of $T_{\downarrow \text{edge } e}$ is $\mathcal{L}(T)$, and the split set of $T_{\downarrow \text{edge } e}$ is $\mathcal{S}(T) \setminus \{A|B\}$, where $A|B$ is the split induced by edge e .

2.2. Poset preliminaries. *Poset.* A poset $\mathcal{P} := (P, \preceq)$ is a tuple where P is a collection of elements and \preceq is a binary relation, satisfying the following properties: (i) reflexivity: $x \preceq x$, $\forall x \in P$; (ii) transitivity: $x \preceq y, y \preceq z \Rightarrow x \preceq z$, $\forall x, y, z \in P$; and (iii) anti-symmetry: $x \preceq y, y \preceq x \Rightarrow x = y$, $\forall x, y \in P$.

Covering relationships. An element $y \in P$ covers $x \in P$ if $x \preceq y$, $x \neq y$, and there is no $z \in P \setminus \{x, y\}$ with $x \preceq z \preceq y$; we call such (x, y) a *covering pair*.

Path. A path from $x_1 \in P$ to $x_k \in P$ is a sequence (x_1, \dots, x_k) with $x_2, \dots, x_{k-1} \in P$ such that x_i covers x_{i-1} for each $i = 2, \dots, k$.

Least element. A poset has a *least element* $x_{\text{least}} \in P$ such that $x_{\text{least}} \preceq y$ for all $y \in P$. By the anti-symmetry property of posets, a least element (if it exists) is unique.

Maximal element. An element $x \in P$ is maximal if there does not exist a distinct element $y \in P$ with $x \preceq y$.

Gradedness. A poset with a least element x_{least} is *graded* if there exists a function $\text{rank} : P \rightarrow \mathbb{N}$ mapping poset elements to the nonnegative integers such that $\text{rank}(y) = \text{rank}(x) + 1$ for any $y \in P$ that covers $x \in P$, and $\text{rank}(x_{\text{least}}) = 0$.

Subposet. The poset $\mathcal{P}_{\text{sub}} := (P_{\text{sub}}, \preceq)$ is a *subposet* of \mathcal{P} when $P_{\text{sub}} \subseteq P$.

3. PROPOSED POSET FRAMEWORK

3.1. A flexible tree space organized via a poset. Let \mathcal{X} be the complete set of leaf labels under consideration; any given tree may have leaf labels $X \subseteq \mathcal{X}$. Define T_0 as the set of all completely unresolved (star) trees whose leaf set is any subset $X \subseteq \mathcal{X}$ and whose split set is empty. Now define the set

$$\mathcal{T} = T_0 \cup \{T : T \text{ is a tree with } \mathcal{L}(T) \subseteq \mathcal{X}, \mathcal{S}(T) \neq \emptyset, \text{ and degree of every internal node } \geq 3\}.$$

This set consists of (i) the special element T_0 , representing all unresolved trees; and (ii) all trees whose leaves are a subset of \mathcal{X} , whose split set is non-empty, and whose internal nodes have degree at least three. We impose the latter constraint to ensure that the trees represent a valid topology for a phylogenetic tree. Each such tree T with $\mathcal{S}(T) \neq \emptyset$ is treated as a distinct element of \mathcal{T} .

The flexibility of \mathcal{T} is highlighted by two features. Firstly, trees are not required to be binary, allowing for varying degrees of resolution in the set of trees. In addition, trees are not required to have the full leaf set \mathcal{X} ; they may be missing leaves. In this way, \mathcal{T} encompasses a diverse collection of tree topologies.

Trees in \mathcal{T} vary in their complexity: more complex trees have more features, i.e. more leaves and more edges. However, only certain trees are directly comparable in their complexity. For example, adding a new leaf to a tree adds complexity. Similarly, refining an unresolved internal node through the addition of a split also adds complexity. We formalize this concept of tree complexity through a binary relation on \mathcal{T} .

Define the tuple $\mathcal{P} := (\mathcal{T}, \preceq)$ consisting of elements \mathcal{T} and a binary relation \preceq on this set, where $T_0 \preceq T_a$ for all $T_a \in \mathcal{T}$, and for any $T_a, T_b \in \mathcal{T} \setminus \{T_0\}$, we define $T_a \preceq T_b$ if $\mathcal{L}(T_a) \subseteq \mathcal{L}(T_b)$ and $\mathcal{S}(T_a) \subseteq \Phi_{\mathcal{L}(T_a)}(\mathcal{S}(T_b))$. This tuple defines a poset, as formalized below and proven in Appendix A.1.

Theorem 1. *The tuple $\mathcal{P} := (\mathcal{T}, \preceq)$ forms a poset with the least element T_0 . In this poset, for any two trees $T_a, T_b \in \mathcal{T} \setminus \{T_0\}$, the tree T_b covers T_a if and only if either (i) $\mathcal{L}(T_a) = \mathcal{L}(T_b)$, $\mathcal{S}(T_a) \subseteq \mathcal{S}(T_b)$ and $|\mathcal{S}(T_b) \setminus \mathcal{S}(T_a)| = 1$; or (ii) $\mathcal{L}(T_a) \subseteq \mathcal{L}(T_b)$, $\Phi_{\mathcal{L}(T_a)}(\mathcal{S}(T_b)) = \mathcal{S}(T_a)$ and $|\mathcal{L}(T_b) \setminus \mathcal{L}(T_a)| = 1$. Moreover, a tree T_b covers T_0 if and only if it has exactly four leaves and a single internal edge.*

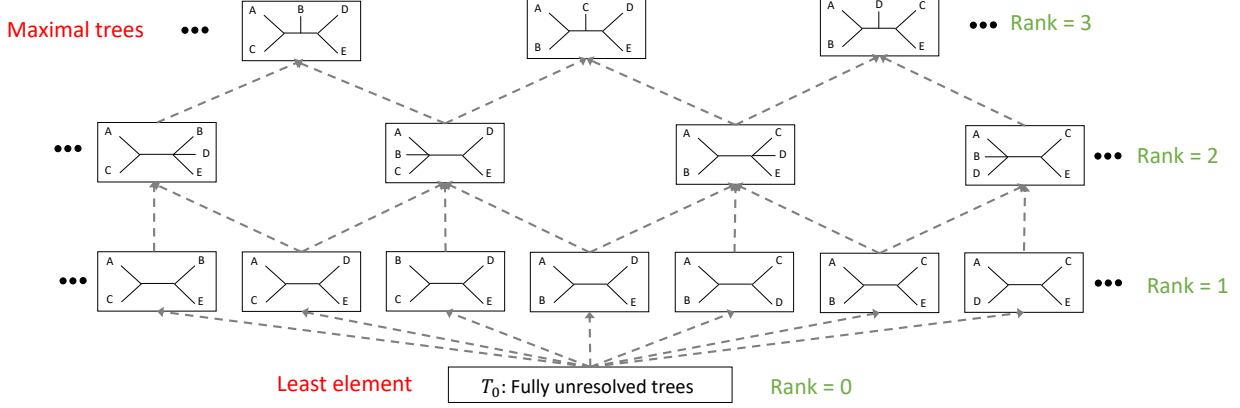


FIGURE 1. A subset of the Hasse diagram for tree space over leaf set $\{A, B, C, D, E\}$.

The partial order \preceq on the set \mathcal{T} captures how trees relate to one another in terms of informational content. In this structure, a tree T_a is considered less than or equal to a tree T_b (i.e., $T_a \preceq T_b$) if and only if all the features in T_a are ‘contained’ in T_b ; that is, the leaf set of T_a is contained in the leaf set of T_b , and the split set of T_a are contained in those of T_b (after restricting T_b ’s leaf set). Intuitively, this means that T_b contains all the information present in T_a , and possibly more. The covering relation in this poset represents the smallest possible refinement to a tree’s structure: either through the addition of a single new split or the inclusion of one additional leaf while preserving all existing relationships. In this way, the poset provides a hierarchical organization of all trees on subsets of \mathcal{X} , ordered by how much structural information they encode.

The special element T_0 serves as the least element in this structure. It represents all completely unresolved trees, and is below every other element in the poset. Any tree with at least one split – no matter how small or incomplete – contains more structural information than T_0 .

Importantly, not all trees in \mathcal{T} are comparable under the partial ordering. If two trees involve different sets of leaves or incompatible splits, neither is considered greater than nor less than the other. Moreover, the poset \mathcal{P} does not have a unique maximal element. Instead, the maximal elements correspond to fully resolved (i.e., binary) trees over the entire leaf set \mathcal{X} . Note that all trees that cover T_0 in the poset $\mathcal{P} = (\mathcal{T}, \preceq)$ contain a single split with four leaves, since four leaves are the minimum required to define a split in a tree.

Figure 1 shows a subset of the Hasse diagram associated with this poset over five leaves. Each box represents a tree in \mathcal{T} , and each dashed arrow represents a covering relation. That is, we draw $T_1 \dashrightarrow T_2$ if T_2 covers T_1 . If there is a directed path from T_1 to T_2 , we can determine that $T_1 \preceq T_2$. As the cardinality of \mathcal{T} is 29, we show only part of the poset. The poset \mathcal{P} thus naturally specifies a directed acyclic graph, where each node in this graph represents a tree and directed edges encode ordering relationships.

Theorem 2. *The poset $\mathcal{P} = (\mathcal{T}, \preceq)$ is graded with the following rank function for $T \in \mathcal{T}$:*

$$(1) \quad \text{rank}(T) := \begin{cases} |\mathcal{S}(T)| + |\mathcal{L}(T)| - 4 & T \notin T_0, \\ 0 & T \in T_0. \end{cases}$$

We prove this result in Appendix A.2. The rank function reflects the information complexity of a tree, measured by the number of features (splits and leaves) it contains. A greater number of splits indicates a more finely resolved hierarchical structure, while more leaves represent a broader coverage of leaves. The minimal element T_0 is assigned a complexity of zero: given that it is fully unresolved, we view it as containing no information. The subtraction of 4 reflects that a split can only occur when the tree contains four leaves.

This graded structure aligns with our interpretation of \preceq . A larger tree (in a partial order sense) corresponds to a more complex tree, and the rank provides a quantitative measure of the increase in complexity relative to trees in T_0 . The largest possible rank is achieved by a fully resolved (i.e., binary) tree on the full leaf set \mathcal{X} , which has rank $2|\mathcal{X}| - 7$. The rank function thus maps the poset onto $\{0, 1, 2, \dots, 2|\mathcal{X}| - 7\}$, and every

integer in this range corresponds to the rank of at least one tree in the poset. The rank values for the trees in the poset shown in Figure 1 are highlighted alongside each element.

Special case: fixing the leaf set. Let $\mathcal{T}_{\text{fixed-leaf}}$ consist of all trees in \mathcal{T} with leaf set \mathcal{X} . The tuple $\mathcal{P}_{\text{fixed-leaf}} = (\mathcal{T}_{\text{fixed-leaf}}, \preceq)$ forms a subposet of \mathcal{P} , where $T_a, T_b \in \mathcal{T}_{\text{fixed-leaf}}$ satisfy $T_a \preceq T_b$ if $\mathcal{S}(T_a) \subseteq \mathcal{S}(T_b)$. Further, T_b covers T_a if $\mathcal{S}(T_a) \subseteq \mathcal{S}(T_b)$ and $|\mathcal{S}(T_b) \setminus \mathcal{S}(T_a)| = 1$. Finally, the poset $\mathcal{P}_{\text{fixed-leaf}}$ is graded with the rank of a tree given by the number of splits (or equivalently number of internal edges) it contains.

3.2. Measuring maximal commonality between trees. Our ultimate goal is to develop an approach to integrate the information contained in a collection of trees $\mathcal{D} := \{T^{(1)}, T^{(2)}, \dots, T^{(n)}\} \subseteq \mathcal{T}$ into a single summary tree $\hat{T} \in \mathcal{T}$ that reflects features that are well-supported by the collection. Before considering collections of trees, we first define structures – formed by features (splits and leaves) – that are shared by a pair of trees $T_1, T_2 \in \mathcal{T}$. These shared structures are themselves trees, but as their leaf sets may be smaller than the leaf sets of the trees they represent, we refer to them as subtrees. Note that for now, we will use n to denote the sample size; later, we discuss partitioning the data into two sets.

We define shared structure between trees using the partially ordered set $\mathcal{P} = (\mathcal{T}, \preceq)$. Specifically, a common subtree between T_1 and T_2 is naturally defined as a tree $T \in \mathcal{T}$ such that $T \preceq T_1$ and $T \preceq T_2$. The ordering ensures that every leaf in T is present in both T_1 and T_2 , and every split in T is supported by both T_1 and T_2 . Among all such common subtrees, those of maximal complexity – as measured by the function $\text{rank}(\cdot)$ in (8) – capture the most complex shared structure. The complexity of these maximal common subtrees quantifies the overall shared similarity. This leads to the following definition.

Definition 1 (Maximal common subtree and similarity). *A maximal common tree between a pair of trees $T_1, T_2 \in \mathcal{T}$ is any maximizer:*

$$(2) \quad T_c \in \underset{T \in \mathcal{T}, T \preceq T_1, T \preceq T_2}{\operatorname{argmax}} \text{rank}(T).$$

The set of maximal common trees are denoted by $\mathcal{M}(T_1, T_2)$. Further, the amount of similarity between trees $T_1, T_2 \in \mathcal{T}$ is measured as

$$(3) \quad \rho(T_1, T_2) := \text{rank}(T_c) = \max_{T \in \mathcal{T}, T \preceq T_1, T \preceq T_2} \text{rank}(T).$$

The set of maximal common trees $\mathcal{M}(T_1, T_2)$ need not be a singleton. Moreover, a maximal common tree may omit some leaves even when they are shared by both input trees, as illustrated in Figure 2.

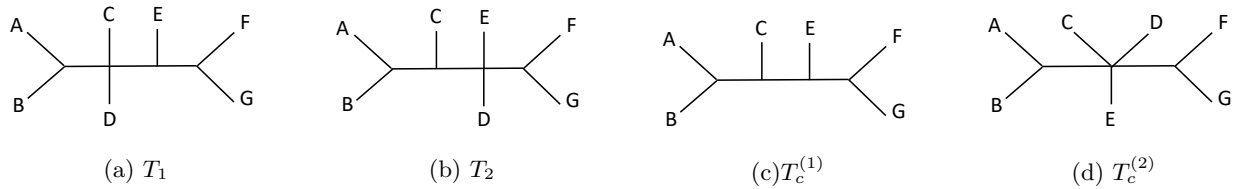


FIGURE 2. Let $\mathcal{X} = \{A, B, C, D, E, F, G\}$ and consider the above trees in \mathcal{T} . Both $T_c^{(1)}$ and $T_c^{(2)}$ are maximal common trees of T_1 and T_2 , and $\rho(T_1, T_2) = \text{rank}(T_c^{(1)}) = \text{rank}(T_c^{(2)}) = 5$. In $T_c^{(1)}$, the leaf D is not present, while $T_c^{(2)}$ lacks the internal edge that induces inconsistent splits across T_1 and T_2 .

The similarity function ρ has a number of desirable properties. First, for any $T_1, T_2 \in \mathcal{T}$, $0 \leq \rho(T_1, T_2) \leq \min\{\text{rank}(T_1), \text{rank}(T_2)\}$, that is, the similarity is non-negative and never exceeds the complexity of either tree. Second, the similarity function satisfies $\rho(T_1, T_2) = \text{rank}(T_1)$ if and only if $T_1 \preceq T_2$. In other words, the similarity function achieves the upper bound if and only if one tree is a subtree of the other. Finally, for any trees $T_1, T_2, T_3 \in \mathcal{T}$ with $T_1 \preceq T_3$, $\rho(T_1, T_2) \leq \rho(T_3, T_2)$. This property ensures that the similarity measures respects the partial order structure, such that larger trees lead to higher similarity.

In Appendix B, we describe an algorithm to compute the similarity function ρ for any pair of trees. The computation begins by identifying all common splits induced by the edges in both trees pairwise, removing leaves that make them incongruent. The similarity is then the maximum rank of any tree that can be reconstructed from a subset of these common splits, retaining only leaves present in every split in the subset. All valid subsets of these common splits are explored iteratively.

3.3. Evaluating true and false discoveries. Having defined a measure of similarity between trees in (3), we can define true and false discoveries of one tree \hat{T} with respect to another tree T^* . Our definitions of true and false discoveries are agnostic to the relationship between \hat{T} and T^* ; indeed, no relationship needs to exist for these quantities to be well-defined. However, when we present a procedure for constructing a \hat{T} that controls the FDR, we will consider \hat{T} to be an estimator ($\hat{T} = \hat{T}(T^{(1)}, \dots, T^{(n)})$) where $T^{(\ell)} \stackrel{iid}{\sim} F$ where F is some unknown data distribution and T^* is some summary of the data distribution (i.e., $T^* = T^*(F)$).

Using our similarity function ρ , we apply the framework in Taeb et al. (2024), which defines true and false discoveries as well as the false discovery proportion for a graded poset.

Definition 2. We define the number of true discoveries, false discoveries and false discovery proportion of $\hat{T} \in \mathcal{T}$ with respect to $T^* \in \mathcal{T}$ as

$$\begin{aligned} \text{TD}(\hat{T}, T^*) &:= \rho(\hat{T}, T^*), \\ \text{FD}(\hat{T}, T^*) &:= \text{rank}(\hat{T}) - \rho(\hat{T}, T^*) = \text{rank}(\hat{T}) - \text{TD}(\hat{T}, T^*), \\ \text{FDP}(\hat{T}, T^*) &:= \frac{\text{rank}(\hat{T}) - \rho(\hat{T}, T^*)}{\text{rank}(\hat{T})} = \frac{\text{FD}(\hat{T}, T^*)}{\text{rank}(\hat{T})}. \end{aligned} \tag{4}$$

Here, the functions $\rho(\cdot, \cdot)$ and $\text{rank}(\cdot)$ are defined in (3) and (8), respectively. We use the convention $0/0 = 0$.

Note that with false discovery proportion defined, we can obtain an analog of the false discovery rate (Benjamini & Hochberg 1995) for trees:

$$\text{FDR} := \mathbb{E}[\text{FDP}(\hat{T}, T^*)],$$

where the expectation is over the randomness in the estimate \hat{T} .

The number of true discoveries $\text{TD}(\hat{T}, T^*)$ is measured as the similarity between \hat{T} and T^* . The number of false discoveries is measured as the complexity of the estimated tree minus the number of true discoveries. Finally, false discovery proportion is the number of false discoveries incurred by the estimate, normalized by its complexity.

The properties of the similarity function ρ result in multiple desirable properties. Firstly, the number of true or false discoveries is non-negative and never exceeds the complexity of the estimated or reference tree, and the false discovery proportion lies in the interval $[0, 1]$. In addition, larger estimates (in a partial order sense) result in larger amount of true discoveries, and the number of false discoveries is equal to zero if and only if $\hat{T} \preceq T^*$, that is, the estimated tree is a subtree of the reference tree.

The number of false discoveries $\text{FD}(\hat{T}, T^*)$ is precisely the number of extra leaves or splits in \hat{T} relative to any maximal common tree between \hat{T} and T^* . This is a more sophisticated measure of false discoveries than the count of the extra leaves and splits that \hat{T} contains relative to T^* , i.e., $|\Phi_{\mathcal{L}(\hat{T}) \cap \mathcal{L}(T^*)}(\mathcal{S}(\hat{T})) \setminus \Phi_{\mathcal{L}(\hat{T}) \cap \mathcal{L}(T^*)}(\mathcal{S}(T^*))| + |\mathcal{L}(\hat{T}) \setminus \mathcal{L}(T^*)|$, as we illustrate in the following example.

Example 3. Consider the trees \hat{T}, T^* and the maximal common subtree T_c between them in Figure 3. Here, $\rho(\hat{T}, T^*) = 1$ as \hat{T} contains one additional leaf as compared to T_c . The naive approach of counting excess leaves and splits yields an error of three (three incorrect splits). The naive approach overcounts false discoveries: removing leaf C from \hat{T} yields the same splits as T^* .

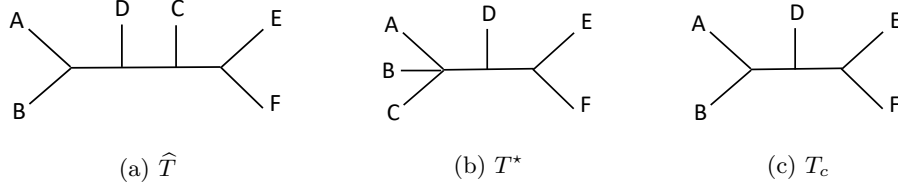


FIGURE 3. Trees associated with Example 3.

4. STABLE CONSENSUS TREE ESTIMATION

Suppose we have access to tree samples $\mathcal{D} := \{T^{(\ell)}\}_{\ell=1}^n \subseteq \mathcal{T}$. Our objective is to identify a stable consensus tree – a tree whose features (internal edges and leaves) are consistently supported across the samples. In Section 4.1, we define the stability of a leaf and the stability of an edge in a reference tree $T \in \mathcal{T}$, relative to the samples \mathcal{D} . With the definitions of stability in place, in Section 4.2, we present an algorithm for selecting a stable tree (with stable leaves and edges) from the samples

Recall, throughout, that $E(T)$ denotes the set of edges in T , S_e is the split associated with an edge $e \in E(T)$, and $\mathcal{M}(T, T^{(\ell)})$ refers to the set of maximal common subtrees shared between T and $T^{(\ell)}$, as defined in Definition 1.

4.1. Measuring stability. We are interested in quantifying how stable each leaf in T is, relative to the collection of tree samples $\mathcal{D} := \{T^{(\ell)}\}_{\ell=1}^n$. Consider a leaf $a \in \mathcal{L}(T)$. One might be tempted to define the stability of leaf a simply as $\frac{1}{|\mathcal{D}|} \sum_{T^{(\ell)} \in \mathcal{D}} \mathbb{I}[a \in \mathcal{L}(T^{(\ell)})]$, which measures the proportion of samples in which a appears as a leaf. However, this definition fails to account for the position of a in the tree T . For example, in the case where the samples have the same leaf set, one could artificially insert all leaves from the samples into T at arbitrary positions, thereby achieving a stability score of one for every leaf. As a result, this alternative notion of stability can yield misleading or meaningless values. Since our model space allows for trees with varying leaf sets, a more meaningful measure of stability is needed, which we define next.

Definition 3. (*Leaf stability*) Let $\mathcal{D} := \{T^{(\ell)}\}_{\ell=1}^n \subseteq \mathcal{T}$ be a collection of tree samples, and let $T \in \mathcal{T}$. The stability of a leaf $a \in \mathcal{L}(T)$ is defined as the proportion of samples for which the similarity between the tree T with leaf a removed, and the sample is lower than the similarity between the full tree T and the sample:

$$(5) \quad \pi_{\text{leaf}, \mathcal{D}}(a; T) := \frac{1}{|\mathcal{D}|} \sum_{T^{(\ell)} \in \mathcal{D}} \mathbb{I} \left[\rho(T_{\downarrow \text{leaf } a}, T^{(\ell)}) < \rho(T, T^{(\ell)}) \right] \in [0, 1].$$

Here, $T_{\downarrow \text{leaf } a}$ is the tree T with leaf a removed; see Section 2.1.

Note that $T_{\downarrow \text{leaf } a} \preceq T$. By the monotonicity property of the similarity function, it follows that $\rho(T_{\downarrow \text{leaf } a}, T^{(\ell)}) \leq \rho(T, T^{(\ell)})$. Thus, the stability score $\pi_{\text{leaf}, \mathcal{D}}(a; T)$ measures how often the similarity strictly decreases when leaf a is removed – that is, how often leaf a contributes positively to the overall similarity with the samples.

If leaf a is not present in the sample $T^{(\ell)}$ (i.e., $a \notin \mathcal{L}(T^{(\ell)})$), it follows that removing a from T does not affect its similarity with the sample. That is, $\rho(T_{\downarrow \text{leaf } a}, T^{(\ell)}) = \rho(T, T^{(\ell)})$. In other words, $a \in \mathcal{L}(T^{(\ell)})$ is a necessary condition for the similarity with $T^{(\ell)}$ to increase when comparing T with and without the leaf a . However, the condition $a \in \mathcal{L}(T^{(\ell)})$ is not sufficient. The following provides a precise characterization.

Lemma 4. The condition $\rho(T_{\downarrow \text{leaf } a}, T^{(\ell)}) < \rho(T, T^{(\ell)})$ is equivalent to requiring $a \in \mathcal{L}(\tilde{T})$ for all $\tilde{T} \in \mathcal{M}(T, T^{(\ell)})$, where $\mathcal{M}(T, T^{(\ell)})$ denotes the set of maximal common subtrees between T and $T^{(\ell)}$.

This lemma, proven in Appendix A.3, states that unlike $\mathbb{I}[a \in \mathcal{L}(T^{(\ell)})]$, which simply checks whether a appears as a leaf in the sample $T^{(\ell)}$, $\rho(T_{\downarrow \text{leaf } a}, T^{(\ell)}) < \rho(T, T^{(\ell)})$ imposes a strictly stronger requirement: that a be present in every maximal common subtree between T and $T^{(\ell)}$. If this condition is not met, leaf a is considered irrelevant for that sample. Thus, our measure $\pi_{\text{leaf}, \mathcal{D}}(a; T)$ not only quantifies how often the leaf a appears in the samples, but also how consistently it is preserved in the shared parts of the trees.

Now consider an internal edge $e \in E(T)$ that induces a non-trivial split. To quantify its stability, a seemingly reasonable strategy is to compute $\frac{1}{|\mathcal{D}|} \sum_{T^{(\ell)} \in \mathcal{D}} \mathbb{I}[S_e \in \Phi_{\mathcal{L}(T)}(\mathcal{S}(T^{(\ell)}))]$, which measures the proportion of samples in which the split S_e , induced by e , appears among the splits of $T^{(\ell)}$ after restricting to the leaf set of T . With this measure, if the edge e implies any separations that are not consistent with $\mathcal{T}^{(\ell)}$, then $\mathbb{I}[S_e \in \Phi_{\mathcal{L}(T)}(\mathcal{S}(T^{(\ell)}))]$ is equal to zero, regardless of how many other leaves in T are separated in the same way as in $T^{(\ell)}$. Thus, this measure does not account for the fact that, by dropping some leaves from T , certain separations associated with the edge e may be preserved in the resulting subtree and become consistent with the separations in the sample $T^{(\ell)}$.

Our flexible model space accommodates trees with arbitrary leaf sets, enabling a more appropriate notion of edge stability.

Definition 4. (*Edge stability*) Let $\mathcal{D} := \{T^{(\ell)}\}_{\ell=1}^n \subseteq \mathcal{T}$ be a collection of tree samples, $T \in \mathcal{T}$, and $e \in E(T)$ be an internal edge. The stability of e is defined as the proportion of tree samples for which the similarity between the tree T with edge e collapsed, and the sample is lower than the similarity between the full tree T and the sample:

$$(6) \quad \pi_{\text{edge}, \mathcal{D}}(e; T) := \frac{1}{|\mathcal{D}|} \sum_{T^{(\ell)} \in \mathcal{D}} \mathbb{I} \left[\rho(T_{\downarrow \text{edge } e}, T^{(\ell)}) < \rho(T, T^{(\ell)}) \right] \in [0, 1].$$

Here, $T_{\downarrow \text{edge } e}$ is the tree after removing edge e from T ; see Section 2.1.

Note that $T_{\downarrow \text{edge } e} \preceq T$. By the monotonicity property of the similarity function, we have that $\rho(T_{\downarrow \text{edge } e}, T^{(\ell)}) \leq \rho(T, T^{(\ell)})$. Thus, the stability score $\pi_{\text{edge}, \mathcal{D}}(e; T)$ measures how often the similarity strictly decreases when the edge e is collapsed – that is, how often the edge e contributes positively to the overall similarity with the samples.

To better understand what the condition $\rho(T_{\downarrow \text{edge } e}, T^{(\ell)}) < \rho(T, T^{(\ell)})$ means, we obtain an equivalent characterization. Our characterization requires the following definition.

Definition 5 (Separating leaf-subsets). Let $A|B$ denote the split specified by edge e in tree T . We define the set of leaf-subsets that separate e from the neighboring edges in T as:

$$U_T(e) := \{A \Delta A' \mid \text{for some } e' = (A'|B') \in E(T) \text{ adjacent to } e \text{ with } A \subset A' \text{ or } A' \subset A\},$$

where $A \Delta A'$ is the symmetric difference of sets A and A' .

The set $U_T(e)$ contains all minimal sets of leaves that would need to be removed from T so that two edges in T map to the same one in the modified tree.

Lemma 5. The condition $\rho(T_{\downarrow \text{edge } e}, T^{(\ell)}) < \rho(T, T^{(\ell)})$ is equivalent to requiring that for all $\tilde{T} \in \mathcal{M}(T, T^{(\ell)})$, there exists $e' \in E(\tilde{T})$ with associated split $S_{e'} = (A'|B')$ such that $\Phi_{\mathcal{L}(\tilde{T})}(A|B) = A'|B'$, where $S_e = (A|B)$ is the associated split to e , and for all leaf-subsets $\mathcal{L}' \in U_T(e)$, $\mathcal{L}' \cap \mathcal{L}(\tilde{T}) \neq \emptyset$.

We prove this lemma in Appendix A.5. This lemma states that unlike $\mathbb{I}[S_e \in \Phi_{\mathcal{L}(T)}(\mathcal{S}(T^{(\ell)}))]$, which simply checks whether all leaf separations implied by edge in T are also implied by $T^{(\ell)}$, $\rho(T_{\downarrow \text{edge } e}, T^{(\ell)}) < \rho(T, T^{(\ell)})$ imposes the condition that *every* maximal common subtree between T and $T^{(\ell)}$ contains some edge that can only come from split $(A|B)$ in T . If this condition is not met, edge e is considered irrelevant for that sample. Thus, in words, $\pi_{\text{edge}, \mathcal{D}}(e; T)$ quantifies how consistently the ‘structural signal’ of the edge e – as defined by the leaf-subsets that separates it from the other edges – is preserved across all maximal common subtrees shared with the tree samples.

Definitions 3 and 4 naturally lead to a notion of stability for a tree, as defined next.

Definition 6. (α -stable consensus tree) A tree $T \in \mathcal{T}$ is called an α -stable tree for $\alpha \in (0, 1]$ if all its features are α -stable. That is:

$$\pi_{\text{edge}, \mathcal{D}}(e; T) \geq \alpha \quad \forall e \in E(T) \quad \text{and} \quad \pi_{\text{leaf}, \mathcal{D}}(a; T) \geq \alpha \quad \forall a \in \mathcal{L}(T).$$

Goal: Given stability threshold $\alpha \in (0, 1]$, identify an α -stable consensus tree $T \in \mathcal{T}$.

Naturally, it is desirable to obtain a tree that is not only α -stable but also complex. We next describe a strategy that prioritizes trees with higher rank (i.e., greater complexity) when identifying α -stable trees.

4.2. Selecting a stable consensus tree. Recall the objective described in the previous section. Our approach traverses the poset \mathcal{P} and proceeds as follows. Starting from the least element of the poset, we greedily grow a path in which each successive tree (that covers the previous one) is α -stable. If the greedily selected successor is not α -stable, we use Definitions 3–4 to compute the stability values of all its features. We then rank these features from least to most stable and choose the first one that does not correspond to the newly added feature (relative to the previously stable tree), removing it to obtain a modified tree. If the resulting tree is still not α -stable, we continue removing the least stable features until it is. Once the tree becomes α -stable again, we repeat the process: grow the tree and remove features if necessary. We summarize the procedure in Algorithm 1.

Algorithm 1 Stable Consensus Tree Estimation

```

1: Input: Poset  $\mathcal{P} = (\mathcal{T}, \preceq)$ , samples  $\mathcal{D} := \{T^{(1)}, \dots, T^{(n)}\} \subseteq \mathcal{T}$ , stability threshold  $\alpha \in (0, 1]$ .
2: Initialize:  $T_u \leftarrow T_0$ 
3: while true do
4:    $\mathcal{C} \leftarrow \{T_v \in \mathcal{T} : T_v \text{ covers } T_u\}$ 
5:   Sort  $\mathcal{C}$  by  $\text{score}_{\mathcal{D}}(T_u, T_v)$  (descending)
6:    $T_v \leftarrow$  first tree in  $\mathcal{C}$ , in order, that is  $\alpha$ -stable
7:   if  $T_v$  exists then
8:      $T_u \leftarrow T_v$ 
9:   else
10:    For first  $T_v \in \mathcal{C}$  do:
11:       $\mathcal{F} \leftarrow$  features of  $T_v$  not added from  $T_u$ , sorted by stability (ascending)
12:      for feature  $f \in \mathcal{F}$  sequentially do
13:        Remove  $f$  from  $T_v$  to get  $T'_v$ 
14:        if  $T'_v$  is  $\alpha$ -stable then
15:           $T_u \leftarrow T'_v$ 
16:          break if statement and continue with while loop
17:        end if
18:      end for
19:      break: terminate and go to step 22
20:    end if
21: end while
22: Output:  $\hat{T} = T_u$ 

```

More concretely, when ranking trees T_v that cover T_u (step 5 of Algorithm 1), we use the following score function:

$$(7) \quad \text{score}_{\mathcal{D}}(T_u, T_v) := \frac{1}{|\mathcal{D}|} \sum_{T^{(\ell)} \in \mathcal{D}} \mathbb{I} \left[\rho(T_u, T^{(\ell)}) < \rho(T_v, T^{(\ell)}) \right],$$

The function $\text{score}_{\mathcal{D}}(T_u, T_v)$ computes how much the additional component introduced by T_v relative to T_u (i.e., a leaf or an edge) is supported by the tree samples. Note that if T_v has an additional leaf a compared to T_u , then $\text{score}_{\mathcal{D}}(T_u, T_v) = \pi_{\text{leaf}, \mathcal{D}}(a; T_v)$. On the other hand, if T_v has an additional edge e compared to T_u , then $\text{score}_{\mathcal{D}}(T_u, T_v) = \pi_{\text{edge}, \mathcal{D}}(e; T_v)$.

The connection of the score function with the stability measures $\pi_{\text{leaf}, \mathcal{D}}$ and $\pi_{\text{edge}, \mathcal{D}}$ means that $\text{score}_{\mathcal{D}}(T_u, T_v) \geq \alpha$ a sufficient (though not necessary) condition for v to be α -stable. While the algorithm prioritizes candidates based on the stability of the added component, it still explicitly verifies the stability of the entire tree before selecting T_v .

Example 6. Consider a multispecies coalescent model (Rannala & Yang 2003) in Figure 4(a) among species $\{A, B, C, D, E, F, G\}$. Here, each internal node represents a speciation event, the numbers represent time

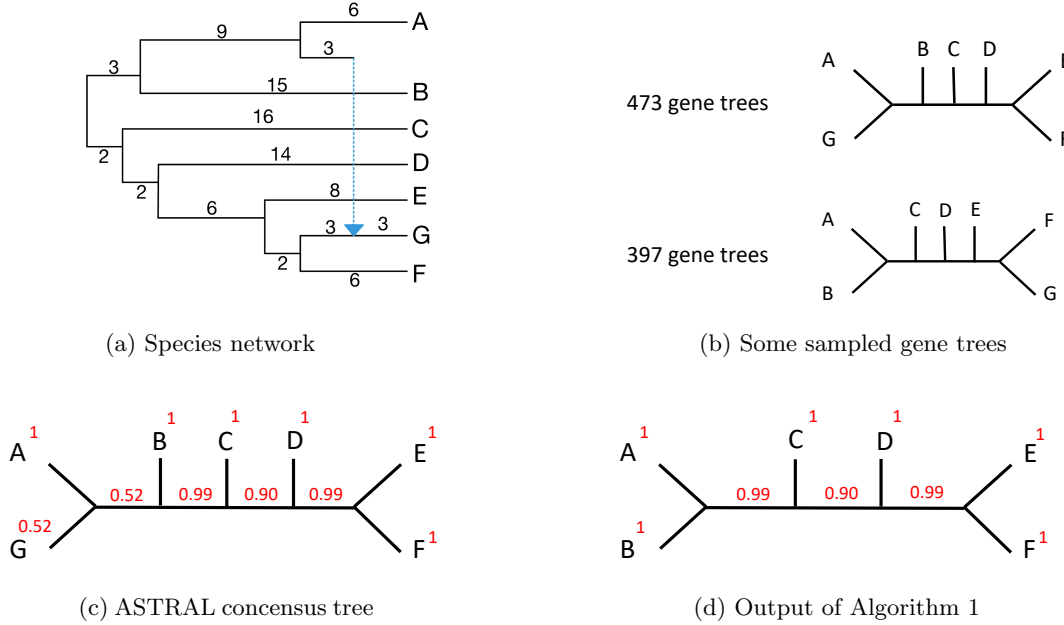


FIGURE 4. (a) Species network that generates gene trees according to a multispecies coalescent model with blue dotted line representing a process known as species ‘hybridization’; (b) Some of the sampled gene trees among $n = 1000$ samples; (c) The tree obtained by the quartet maximization estimator ASTRAL (Mirarab et al. 2014), and the stability of each of its features as computed by Definitions 3-4 (shown in red); and (d) The tree obtained by Algorithm 1 with $\alpha = 0.9$, and the stability value of each of its features.

between speciation events, and the dotted blue lines is a hybridization event representing genetic mixing (hybridization probability is set to be 0.52). We generate $n = 1000$ gene trees from this species network, where the majority of the trees are the two shown in Figure 4(b). Supplying the samples to the procedure called ASTRAL (Mirarab et al. 2014) produces the tree in Figure 4(c). Despite the significant uncertainty in the placement of leaf G, ASTRAL produces a fully resolved tree with all the leaves present. The stability of its features, as computed via measures in Definitions 3-4, are shown in red, highlighting how multiple of its features have low stability values. Figure 4(d) shows the output of Algorithm 1 with $\alpha = 0.9$. As desired, leaf G is dropped, as its location is highly varied in the samples. Further, feature stability values (shown in red) are all high.

5. FALSE DISCOVERY RATE CONTROL GUARANTEES

In this section, we provide a strategy for tree selection that controls the FDR. Specifically, let T^* denote a fixed data-independent reference tree; see the discussion in Section 3.3. For a desired user-specified threshold $q \in (0, 1)$, we output a tree \hat{T} satisfying $\mathbb{E}[\text{FDP}(\hat{T}, T^*)] \leq q$. As discussed later in the section, existing algorithms in the multiple testing literature are not appropriate for this problem, and hence we develop a new procedure.

In Section 5.1, we provide some preliminary discussion, including the need for reducing the search space using a subposet \mathcal{P}_{sub} . In Section 5.2, we present an algorithm for tree selection with respect to a given subposet \mathcal{P}_{sub} . We show in Section 5.3 that our algorithm controls the FDR. Motivated by this theoretical result, we discuss in Section 5.4 a strategy for selecting the subposet \mathcal{P}_{sub} .

5.1. Preliminaries. The number of trees in the collection \mathcal{T} can be massive. For example, when $|\mathcal{X}| = 6$ (i.e., 6 leaves), $|\mathcal{T}| = 1055$; when $|\mathcal{X}| = 7$, $|\mathcal{T}| = 28,704$; and when $|\mathcal{X}| = 8$, $|\mathcal{T}| = 1,066,275$! This explosive growth in the model space poses significant statistical challenges. To account for multiplicity while controlling for false discoveries, we must appropriately reduce the search space of models before applying Algorithm 1.

We construct this restricted space as a graded subposet $\mathcal{P}_{\text{sub}} = (\mathcal{T}_{\text{sub}}, \preceq)$ of the poset \mathcal{P} , where $\mathcal{T}_{\text{sub}} \subseteq \mathcal{T}$, and covering pairs in \mathcal{P}_{sub} are also covering pairs in \mathcal{P} .

To motivate our selection strategy, let $\hat{T} \in \mathcal{T}_{\text{sub}}$ be a selected tree. Let $(T_0, T_1, \dots, T_{k-1}, T_k := \hat{T})$ be any path from T_0 to \hat{T} in the subposet \mathcal{P}_{sub} where T_i covers T_{i-1} for every $i = 1, 2, \dots, k$. Here, $k := \text{rank}(\hat{T})$. Then, the false discovery proportion $\text{FDP}(\hat{T}, T^*)$ may be bounded as the following telescoping sum:

$$(8) \quad \text{FDP}(\hat{T}, T^*) = \sum_{i=1}^{\text{rank}(\hat{T})} \frac{1 - [\rho(T_i, T^*) - \rho(T_{i-1}, T^*)]}{\text{rank}(\hat{T})} \leq \sum_{i=1}^{\text{rank}(\hat{T})} \frac{\mathbb{I}[\rho(T_i, T^*) = \rho(T_{i-1}, T^*)]}{\text{rank}(\hat{T})}.$$

Here, the inequality follows from the facts that: (i) by the monotonicity property of the similarity function ρ , since $T_{i-1} \preceq T_i$, we have $\rho(T_{i-1}, T^*) \leq \rho(T_i, T^*)$; and (ii) the difference $\rho(T_i, T^*) - \rho(T_{i-1}, T^*)$ takes on integer values. From (8), we note that $\text{FDP}(\hat{T}, T^*)$ is small when $\rho(T_i, T^*) > \rho(T_{i-1}, T^*)$ for many $i = 1, 2, \dots, \text{rank}(\hat{T})$. Naively, we can thus grow a path in the poset starting from the least element T_0 and adding one element T_i at a time such that the covering pair (T_{i-1}, T_i) satisfy $\rho(T_i, T^*) < \rho(T_{i-1}, T^*)$ often. Since T^* is unknown, for the aforementioned approach to work, we need a data-driven method to control how often $\rho(T_i, T^*) = \rho(T_{i-1}, T^*)$. To that end, a data-driven approach is needed to decide whether we proceed from T_{i-1} to T_i .

5.2. An algorithm for controlling the false discovery rate. We partition our dataset \mathcal{D} , which contains n samples, into two datasets, \mathcal{D}_1 and \mathcal{D}_2 , with n_1 and n_2 samples, respectively, where $n = n_1 + n_2$. We will use the first portion to select a subposet (see Section 5.4); the second portion is used for estimating a tree with FDR control as described next.

Let $r_{\max} := \max_{T \in \mathcal{T}_{\text{sub}}} \text{rank}(T)$ be the complexity of the largest complexity tree in the subposet \mathcal{P}_{sub} . Let \mathcal{M} denote the set of maximal trees in \mathcal{P}_{sub} , i.e.,

$$\mathcal{M} := \{T \in \mathcal{T}_{\text{sub}} : \text{no tree } T' \in \mathcal{T}_{\text{sub}} \text{ covers } T \text{ in } \mathcal{P}_{\text{sub}}\}.$$

We denote $\kappa : \mathcal{T}_{\text{sub}} \rightarrow \mathbb{R}_+$ the function that computes a multiplicity factor for each tree $T \in \mathcal{T}_{\text{sub}}$. Specifically, for each tree $T \in \mathcal{M}$, define $\kappa(T) := |\mathcal{M}| / (\#\text{trees } T \text{ covers in } \mathcal{P}_{\text{sub}})$. For the remaining trees $T \in \mathcal{T}_{\text{sub}}$, we define $\kappa(T)$ recursively, as follows:

$$\kappa(T) := (\#\text{trees } T \text{ covers in } \mathcal{P}_{\text{sub}}) \max_{T' : T' \text{ covers } T \text{ in } \mathcal{P}_{\text{sub}}} \kappa(T').$$

We define a threshold function $\gamma : \mathcal{T}_{\text{sub}} \times [0, 1] \rightarrow [0, 1]$, where for every $T \in \mathcal{T}_{\text{sub}}$ and used-specified FDR threshold $q \in [0, 1]$

$$(9) \quad \gamma(T, q) := \sqrt{\max \left\{ \frac{1}{n_2} \log \left(\frac{\kappa(T) \cdot (r_{\max} - \text{rank}(T) + 1)}{q \cdot r_{\max}} \right), 0 \right\}} + 1/2.$$

The algorithm then proceeds as follows. It initializes $T_u \leftarrow T_0$, the least element of the poset, and iteratively considers all trees $T_v \in \mathcal{T}$ that cover T_u . These candidates are ranked (from largest to smallest) by the score $\text{score}_{\mathcal{D}_2}(T_u, T_v)$, and the algorithm moves to the highest-ranked T_v such that, for every covering pair (T_x, T_y) in \mathcal{P}_{sub} with $T_y \preceq T_v$, $\text{score}_{\mathcal{D}_2}(T_x, T_y) \geq \gamma(T_y, q)$. The algorithm stops when this condition is no longer satisfied. We summarize this procedure in Algorithm 2. Note that when computing the score function in steps 5 and 7 of Algorithm 2, we use the dataset \mathcal{D}_2 . Specifically, $\text{score}_{\mathcal{D}_2}(T_u, T_v) = \frac{1}{|\mathcal{D}_2|} \sum_{T^{(\ell)} \in \mathcal{D}_2} \mathbb{I}[\rho(T_u, T^{(\ell)}) < \rho(T_v, T^{(\ell)})]$.

When moving from tree T_u to T_v , Algorithm 2 does not only check that the score $\text{score}_{\mathcal{D}_2}(T_u, T_v)$ is sufficiently large, but also verifies that, for every path from T_v to the least element T_0 , every covering pair (T_x, T_y) along the path also has a sufficiently large score $\text{score}_{\mathcal{D}_2}(T_x, T_y)$. Note that, by construction, $\kappa(\cdot)$ is a monotonically decreasing function of tree complexity: if $T_1 \preceq T_2$ for $T_1, T_2 \in \mathcal{T}_{\text{sub}}$, then $\kappa(T_2) \leq \kappa(T_1)$. Since the rank function $\text{rank}(\cdot)$ is an increasing function of tree complexity, we conclude that more complex trees T correspond to a smaller threshold $\gamma(T, q)$. This is desirable as more complex trees tend to have smaller scores. Further, as expected, smaller q results in a larger $\gamma(T, q)$ and thus a more stringent threshold requirement.

Relation to existing multiple testing procedures. As described in Section 1.2, traditionally, when developing FDR controlling procedures, the starting point is a collection of hypothesis tests. In settings such as variable selection, it is straightforward to formulate model selection as testing a set of hypotheses over features. However, for tree selection, it is not immediately clear how to construct an analogous family of tests,

because the relevant features (tree edges and leaves) are highly structured: each edge induces a partition only of the leaves present, and not all edges are mutually compatible.

Our poset framework provides a formulation for a hierarchy of hypothesis tests. Specifically, based on the bound in (8), for every covering pair (T_u, T_v) in the subposet \mathcal{P}_{sub} , we can consider the following hypothesis test:

$$H_0(T_u, T_v) : \rho(T_u, T^*) = \rho(T_v, T^*).$$

These hypothesis tests can be organized as vertices in a directed acyclic graph where each vertex is a covering pair (T_u, T_v) and there is a directed path from a vertex (T_u, T_v) to (T'_u, T'_v) if $T_v \preceq T'_u$.

There are existing approaches in the literature that control the FDR when testing a collection of hypotheses organized in a hierarchical structure (G'Sell et al. 2013, Li & Barber 2015, Ramdas et al. 2019, Yekutieli 2008). For a fixed sequence of hypotheses, G'Sell et al. (2013), Li & Barber (2015) design FDR controlling procedures assuming access to independent test statistics across hypotheses. However, deriving independent test statistics in our problem does not seem possible. Note additionally that these procedures could only handle a subposet \mathcal{P}_{sub} that is a chain, where every pair of trees are comparable. Yekutieli (2008) propose a procedure over trees, although their approach again relies on independent test statistics. Ramdas et al. (2019) propose a procedure for hypotheses ordered in a directed acyclic graph. However, their method crucially assumes the Strong Heredity Principle: all parents of a non-null hypothesis are also non-null. In our context, this means that if $H_0(T_u, T_v)$ is truly non-null, then $H_0(T'_u, T'_v)$ is also non-null for all $T'_v \preceq T_u$. This assumption does not generally hold in our setting. Further, in our context, Ramdas et al. (2019) count false discoveries as rejected null hypotheses, whereas the relevant false discoveries in our problem are those associated specifically with a path from T_0 to a selected tree \hat{T} .

The closest approach to what we propose is the method in Lynch et al. (2016). For a fixed sequence of hypotheses, they design a procedure that handles arbitrary dependency among the associated test statistics. When the subposet \mathcal{P}_{sub} is a chain, our method mirrors the one in Lynch et al. (2016). Our method, however, is able to handle an arbitrary subposet \mathcal{P}_{sub} .

Algorithm 2 Tree Selection with False Discovery Rate Control

```

1: Input: Subposet  $\mathcal{P}_{\text{sub}} = (\mathcal{T}_{\text{sub}}, \preceq)$ ; samples  $\mathcal{D}_2$ ; user-specified FDR threshold  $q \in (0, 1)$ ; and stability
   thresholds  $\gamma(\cdot, \cdot)$  set as in (9)
2: Initialize:  $T_u \leftarrow T_0$ 
3: while true do
4:    $\mathcal{C} \leftarrow \{T_v \in \mathcal{T}_{\text{sub}} : v \text{ covers } T_u\}$ 
5:   Sort  $\mathcal{C}$  by  $\text{score}_{\mathcal{D}_2}(T_u, T_v)$  (descending)
6:   for  $T_v \in \mathcal{C}$  do
7:     if for every covering pair  $(T_x, T_y)$  in  $\mathcal{P}_{\text{sub}}$  with  $T_y \preceq T_v$ ,  $\text{score}_{\mathcal{D}_2}(T_x, T_y) \geq \gamma(T_y, q)$  then
8:        $T_u \leftarrow T_v$ 
9:       continue while
10:    end if
11:  end for
12: end while
13: Output:  $\hat{T} = T_u$ 

```

5.3. Theoretical guarantees. To arrive at our guarantees, we first impose the following standard assumption on the tree samples.

Assumption 1. *The tree samples $\{T^{(\ell)} : T^{(\ell)} \in \mathcal{D}_2\}$ are drawn independently and identically from an unknown distribution \mathcal{F} with support \mathcal{T} .*

Assumption 1 is relatively standard in the literature of consensus tree estimation, especially in the context of phylogenetic trees (Allman et al. 2011, 2016, Than & Rosenberg 2011, O'Reilly & Donoghue 2017, Degnan et al. 2008).

Since Algorithm 1 aggregates tree samples drawn from the distribution \mathcal{F} , we expect its performance to rely on how “concentrated” \mathcal{F} is on trees that incur small false discoveries. To make this more precise, consider a fixed summary tree T^* of the data distribution, $T^* = T^*(\mathcal{F})$. Define the set of *null covering pairs*:

$$(10) \quad \mathcal{C}_{\text{null}}(\mathcal{T}_{\text{sub}}, T^*) := \{(T_a, T_b) \in \mathcal{T}_{\text{sub}} \times \mathcal{T}_{\text{sub}} \mid T_b \text{ covers } T_a, \rho(T_a, T^*) = \rho(T_b, T^*)\}.$$

Here, $\mathcal{C}_{\text{null}}(\mathcal{T}_{\text{sub}}, T^*)$ is the set of all covering pairs (T_a, T_b) in the subposet \mathcal{P}_{sub} for which T_b offers *no additional similarity* to the population tree T^* relative to T_a . The following lemma highlights why the covering pair (T_a, T_b) is referred to as a ‘null covering pair’.

Lemma 7. *Consider a pair of covering trees (T_a, T_b) in the subposet \mathcal{P}_{sub} . Then, $\text{FD}(T_b, T^*) > \text{FD}(T_a, T^*)$ if and only if $(T_a, T_b) \in \mathcal{C}_{\text{null}}(\mathcal{T}_{\text{sub}}, T^*)$; that is, T_b incurs additional false discovery relative to T_a if and only if $\rho(T_a, T^*) = \rho(T_b, T^*)$.*

We prove Lemma 7 in Appendix A.4. The following assumption ensures that the distribution \mathcal{F} is not too concentrated on trees that incur some false discoveries.

Assumption 2. *The tree generating distribution \mathcal{F} satisfies*

$$\min_{(T_a, T_b) \in \mathcal{C}_{\text{null}}(\mathcal{T}_{\text{sub}}, T^*)} \mathbb{P}_{T \sim \mathcal{F}} [\rho(T_a, T) = \rho(T_b, T)] \geq 1/2.$$

Here, the term $\mathbb{P}_{T \sim \mathcal{F}} [\rho(T_a, T) = \rho(T_b, T)]$ denotes the probability that, for a null covering pair (T_a, T_b) , a random tree sample T drawn from \mathcal{F} is equally similar (under ρ) to both T_a and T_b . If this probability is large, this means that \mathcal{F} has small mass on trees T that possess strictly more similarity with T_b than with T_a , i.e. those that support growing the tree T_a to T_b even though this will incur additional false discoveries. Assumption 2 states that the minimum such probability among all covering pairs is above one-half.

Theorem 8. *Let T^* be a fixed summary statistic for the data distribution \mathcal{F} . Suppose Assumptions 1-2 hold with \mathcal{T}_{sub} fixed. Algorithm 2 controls the FDR at level q , i.e., $\mathbb{E}[\text{FDP}(\hat{T}, T^*)] \leq q$.*

We prove this theorem in Appendix A.6. We note here that the population tree T^* is not unique with respect to \mathcal{F} . Indeed, Theorem 8 guarantees that if a given T^* satisfies Assumption 2, then our algorithm controls the FDR with respect to T^* .

Remark 1. *Assumption 2 can be replaced with $\min_{(T_a, T_b) \in \mathcal{C}_{\text{null}}(\mathcal{T}_{\text{sub}}, T^*)} \mathbb{P}_{T \sim \mathcal{F}} [\rho(T_a, T) = \rho(T_b, T)] \geq \eta$ for some $\eta \in (0, 1)$. Under this assumption, the threshold in (9) must also be modified, by replacing the term $1/2$ with $1 - \eta$. With this change, the guarantees in Theorem 8 still hold. This implies that if the data generating distribution satisfies the assumption with $\eta > \frac{1}{2}$, then our algorithm with the threshold (9) is more conservative than necessary.*

Remark 2. *Theorem 8 assumes a fixed subposet \mathcal{P}_{sub} with corresponding trees \mathcal{T}_{sub} . A data-driven subposet \mathcal{P}_{sub} can also be considered, as long as the data used to obtain \mathcal{P}_{sub} is separate from the one used in Algorithm 2. Under Assumption 1 and the following adaptation to Assumption 2*

$$\mathbb{E}_{\text{selected } \mathcal{T}_{\text{sub}}} \left(\min_{(T_a, T_b) \in \mathcal{C}_{\text{null}}(\mathcal{T}_{\text{sub}}, T^*)} \mathbb{P}_{T \sim \mathcal{F}} [\rho(T_a, T) = \rho(T_b, T)] \right) \geq \frac{1}{2},$$

we can guarantee FDR control, namely, $\mathbb{E}[\text{FDP}(\hat{T}, T^)] \leq q$, where the expectation is over all randomness, including the selection of \mathcal{T}_{sub} .*

5.4. Search space restriction: selecting subposet \mathcal{P}_{sub} . Motivated by the threshold in (9), we propose a strategy for selecting a subposet \mathcal{P}_{sub} , consisting of trees \mathcal{T}_{sub} . Recall that we split the data \mathcal{D} into \mathcal{D}_1 and \mathcal{D}_2 . We will use \mathcal{D}_1 to construct a subposet \mathcal{P}_{sub} .

Supplying \mathcal{D}_1 to Algorithm 1 with a fixed stability threshold α , we obtain a stable tree \hat{T}_{stable} . We set an anchor rank $r_{\text{anchor}} := \lfloor \log_2 q + n_2(\tau - 1/2)^2 \log_2(e) + 1 \rfloor$ for some $\tau \in (1/2, 1)$, whose choice will be justified later. If the rank of \hat{T}_{stable} is larger than r_{anchor} , we construct a subposet with a structure shown in Figure 5(a).

An upward chain is built from \hat{T}_{stable} to a maximal element in the poset, and a downward chain is constructed to a tree whose rank equals r_{anchor} . Further, from this tree, we bifurcate downward until we reach T_0 . Each tree in the upward or downward path is selected by finding a neighboring tree (one that covers or is covered by the current tree) in the poset that maximizes the score function in (7). The pair of trees used in the bifurcation step is obtained by selecting the two neighboring trees with the highest scores. If the rank of \hat{T}_{stable} is smaller or equal to r_{anchor} , we proceed upwards in a chain from \hat{T}_{stable} to obtain a tree with rank r_{anchor} . From there, we construct a subposet where we proceed greedily upwards (as in the previous case) to a maximal tree, and greedily bifurcate downwards.

We set r_{anchor} so that any tree $T \in \mathcal{T}_{\text{sub}}$ has $\gamma(T, q) \leq \tau$. Note that instead of branching to two trees at each step in the subposet, one can also branch to k trees; with this choice, $r_{\text{anchor}} := \lfloor \log_k q + n_2(\tau - 1/2)^2 \log_k(e) + 1 \rfloor$. Finally, as described in Remark 1, it may be that Assumption 2 is satisfied for a threshold η that is different from $1/2$. In that case, we set $r_{\text{anchor}} := \lfloor \log_2 q + n_2(\tau - \eta)^2 \log_2(e) + 1 \rfloor$.

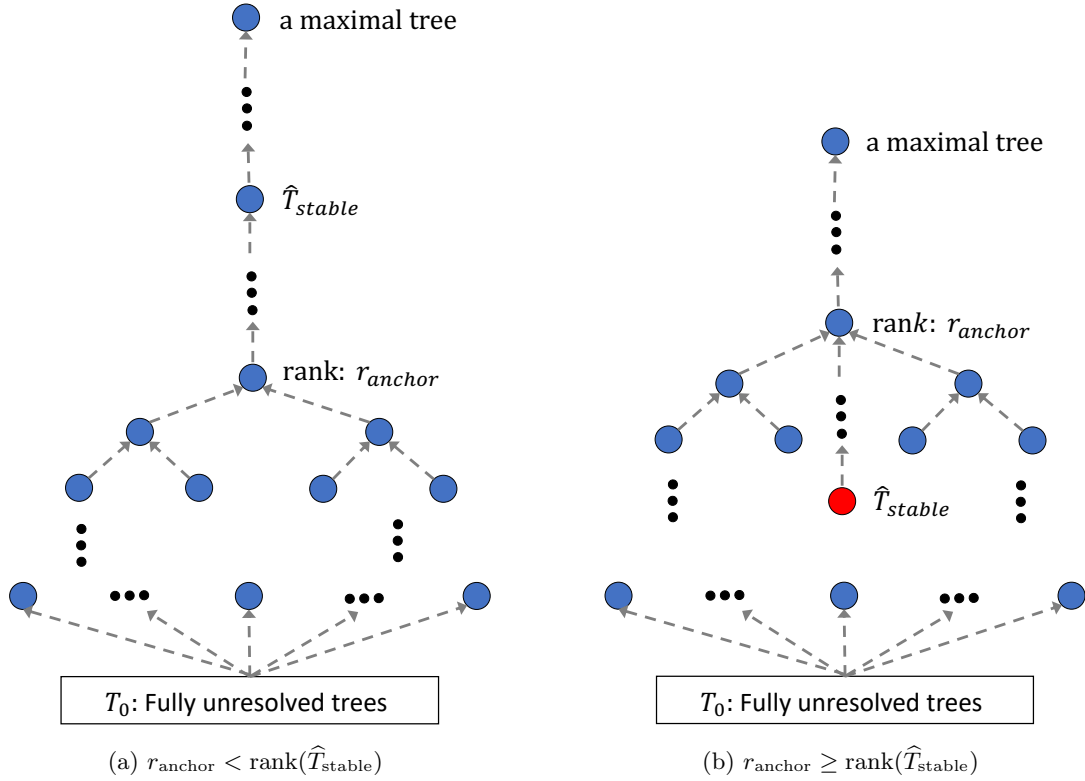


FIGURE 5. The structure of the subposet \mathcal{P}_{sub} in each setting. Here, \hat{T}_{stable} is the output of Algorithm 1, $r_{\text{anchor}} := \lfloor \log_2 q + n_2(\tau - 1/2)^2 \log_2(e) + 1 \rfloor$, and a maximal tree is a tree that is covered by another other tree in \mathcal{P} . Each blue dot represents a tree in the poset \mathcal{P}_{sub} .

6. SIMULATIONS

We now study the true and false discovery rate of our procedure under simulation. We begin by fixing a binary “species tree” T^* on $|\mathcal{X}| = 10$ leaves by selecting a topology uniformly-at-random and assigning edge lengths drawn from a log-normal distribution with arithmetic mean 2 and variance 4 (with log-scale parameters computed accordingly), rounded to the nearest multiple of 0.5. The resulting tree is of rank 13 and contains four edges of length 0.5, and a single branch of length 5.5. Using this species tree as a starting point, we simulate gene trees $\{T^{(1)}, \dots, T^{(n)}\}$ from a multispecies coalescent model (MSC) (Rannala & Yang 2003) under different settings, employing the simulator described in Fogg et al. (2023). All simulations were performed in the default configuration, which implements the modified clockless multispecies coalescent model. In this mode, the simulator places no constraints on population sizes or the number of generations

Algorithm 3 Subposet Selection

```

1: Input: Poset  $\mathcal{P} = (\mathcal{T}, \preceq)$ , samples  $\mathcal{D}_1$  and  $\mathcal{D}_2$  with  $n_2 = |\mathcal{D}_2|$ ; user-specified FDR threshold  $q \in (0, 1)$ ;
   parameter  $\tau \in (1/2, 1]$ ; and stability threshold  $\alpha$ 
2: Apply Algorithm 1 with dataset  $\mathcal{D}_1$  and stability threshold  $\alpha$  to the tree samples to obtain  $\hat{T}_{\text{stable}}$ 
3: Compute  $r_{\text{anchor}} := \lfloor \log_2 q + n_2(\tau - 1/2)^2 \log_2(e) + 1 \rfloor$ 
4: Initialize  $\mathcal{T}_{\text{sub}} \leftarrow T_0$ 
5: if  $\text{rank}(\hat{T}_{\text{stable}}) > r_{\text{anchor}}$  then
6:   Initialize  $T_u \leftarrow \hat{T}_{\text{stable}}$ 
7:   while  $\text{rank}(T_u) < r_{\text{max}}$  do
8:      $\mathcal{C} \leftarrow \{T_v \in \mathcal{T} : T_v \text{ covers } T_u\}$ 
9:     Sort  $\mathcal{C}$  by  $\text{score}_{\mathcal{D}}(T_u, T_v)$  (descending)
10:    Add first element in  $\mathcal{C}$  to  $\mathcal{T}_{\text{sub}}$ 
11:   end while
12:   Initialize  $\mathcal{T}_v \leftarrow \hat{T}_{\text{stable}}$ 
13:   while  $\text{rank}(T_v) > r_{\text{anchor}}$  do
14:      $\mathcal{C} \leftarrow \{T_u \in \mathcal{T} : T_v \text{ covers } T_u\}$ 
15:     Sort  $\mathcal{C}$  by  $\text{score}_{\mathcal{D}}(T_u, T_v)$  (descending)
16:     Add first element in  $\mathcal{C}$  to  $\mathcal{T}_{\text{sub}}$ 
17:   end while
18:   Initialize  $\mathcal{T}_{\text{expand}} \leftarrow T$  where  $T$  is the last  $T_u$  in the previous loop
19:   while  $\mathcal{T}_{\text{expand}} = \emptyset$  do
20:     Take any  $T \in \mathcal{T}_{\text{expand}}$ 
21:      $\mathcal{C} \leftarrow \{T_u \in \mathcal{T} : T \text{ covers } T_u\}$ 
22:     Sort  $\mathcal{C}$  by  $\text{score}_{\mathcal{D}}(T_u, T)$  (descending)
23:     Add first two elements in  $\mathcal{C}$  to  $\mathcal{T}_{\text{sub}}$  and  $\mathcal{T}_{\text{expand}}$ 
24:     Remove  $T$  from  $\mathcal{T}_{\text{expand}}$ 
25:   end while
26: else
27:   Apply steps 6-11 above
28:   Set  $T$  to be tree constructed above with  $\text{rank}(T) = r_{\text{anchor}}$ 
29:   Initialize  $\mathcal{T}_{\text{expand}} \leftarrow T$  and repeat steps 19-25
30: end if
31: Output: Subposet  $\mathcal{P}_{\text{sub}} = (\mathcal{T}_{\text{sub}}, \preceq)$ 

```

along individual branches, and branch lengths are interpreted directly in coalescent units. We wish to estimate the topology of the species tree.

We investigate the effect of two factors on the performance of our procedure: sample size and the lengths of internal branches in the target tree. We expect larger sample sizes to improve estimation performance, whereas shorter internal branches – reflecting high speciation rate – are known to increase genealogical discordance, a phenomenon reflected in the MSC model (Degnan & Rosenberg 2009). For each simulation scenario, we generate n gene trees under the MSC. We use half of these trees ($n_1 = n/2$) to select the α -stable tree with $\alpha = 0.85$ following Algorithm 1, and the remaining half of trees ($n_2 = n/2$) for the final estimation while controlling the FDR using Algorithm 2 across FDR thresholds $q \in \{0.05, 0.10, 0.20, 0.30\}$. In each simulation, we constructed the subposet so that the stability threshold $\gamma(T, q)$ remained below $\tau = 0.75$ for all trees in the subposet. Each simulation setting is replicated 20 times.

We show the impact of varying the number of gene trees n on the number of true discoveries in Figure 6(a). As expected, the ability to resolve the species tree improves as n increases. The number of true discoveries grows with larger values of the false discovery threshold q . Across all simulation scenarios, the number of false discoveries was consistently zero, except for one instance. We incur exactly one false discovery when both the FDR control threshold was high ($q = 0.3$) and the sample size was low ($n = 20$).

The conservatism of the procedure is not surprising. In the proof of Lemma 10, we replace a minimum over a collection of covering pairs with a sum. This leads to an overestimation of the multiplicity factor, driving the

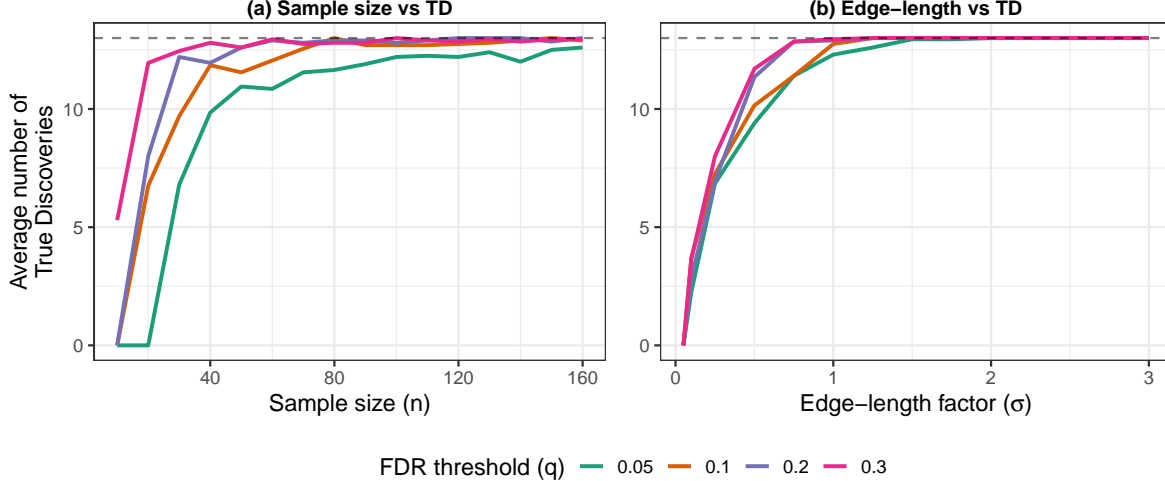


FIGURE 6. Average true discoveries across different sample sizes (a) and different edge-length scales (b). Lines are colored according to the FDR threshold q . The parameter tree has rank 13, which represents the maximum number of true discoveries (indicated by the dashed gray lines).

threshold function γ upward. Consequently, the thresholds required to add a new feature in Algorithm 2 end up stricter than necessary to ensure the FDR remains below q .

We observe the same general behavior when we investigate the impact of altering the branch lengths of T^* for fixed $n = 100$, shown in Figure 6(b). Specifically, we rescaled all branches of T^* by a constant factor σ . Larger branch lengths on the species tree implies greater time between coalescent events and, therefore, greater concentration of the gene trees around the species tree topology. Empirically, we find that the average number of true discoveries increases with σ , while the number of false discoveries remains consistently zero throughout every simulation. This is to be expected, as the ability to resolve relationships in the species tree increases with longer coalescence time.

We also investigate the behavior of feature stabilities in the α -stable trees used in the first stage of the procedure. In all simulations, we constructed stable trees with $\alpha = 0.85$. Since the stability of a feature within a fixed tree depends solely on the sample, we expect the observed stabilities to reflect the relationship between the underlying tree-generating distribution \mathcal{F} and each specific feature in the identified stable tree.

We show the distribution of feature stabilities as \mathcal{F} and n vary in Figure 7. Note that \mathcal{F} is varied by adjusting σ . These stability scores arise from all the features corresponding to the α -stable trees generated in the simulations described above. We also included additional simulations for larger n and σ . In Figure 7(a), we observe that feature stabilities are initially concentrated at 1.0 when the sample size is small. Once the sample includes approximately 20 trees, the stabilities become more dispersed and then gradually increase as n increases. This is consistent with our expectations: for small sample sizes, any feature that is inherently unstable under \mathcal{F} will quickly fall under the threshold, and only strongly supported features will be included in the tree, which inflates the observed stabilities. However, as the sample size increases, the target tree T^* remains fixed while the dataset grows, causing the feature stabilities to converge towards an intrinsic value that is solely dependent on the distribution \mathcal{F} .

When examining feature stabilities across different edge-lengths, we observe that the stabilities begin at relatively low values and increase as σ increases, though variability in the distribution remains. This behavior is expected: under the MSC model, longer internal edges yield more stable features because they reduce the level of incomplete lineage sorting and therefore decrease topological variability in the gene tree distribution. As the internal edge lengths increase, the gene trees sampled from the MSC distribution become less heterogeneous and more closely aligned with the topology of the target tree T^* . Consequently, the features associated with these edges exhibit higher and more consistent stability for large values of σ .

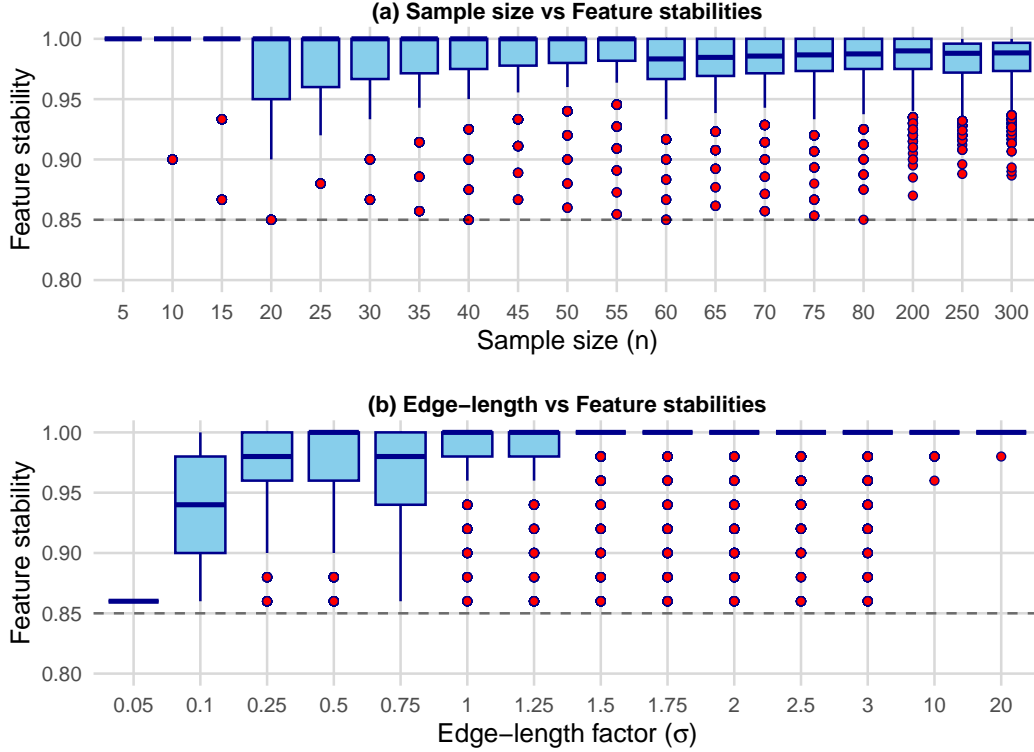


FIGURE 7. Feature stability across different sample sizes (a) and edge-length factor σ (b). Each boxplot summarizes the distribution of stability values across repeated simulations for a given parameter setting. The dashed horizontal line at 0.85 denotes a reference stability threshold.

In summary, our simulation shows (i) as desired, FDR level of our algorithm is under the nominal value q , (ii) the number of true discoveries made by our algorithm increases as the sample size and the edge lengths increase, (iii) the behavior of feature stabilities show that they reflect the distribution \mathcal{F} , and in particular get closer to one as the edge lengths increase, and stabilize as the sample size increases.

7. DATA ANALYSIS: ORIGIN OF EUKARYOTIC LIFE

We now apply our method to investigate the evolutionary origins of complex life. Eukaryotes are believed to have arisen from the entrapment of a bacteria within an archaeon more than two billion years ago (Betts et al. 2018, Imachi et al. 2020), but the closest currently-living relative of the archaeal ancestor of eukaryotic life is unknown. Phylogenetic trees estimated using genes that are shared between archaea and eukaryotes are the best evidence for determining such an ancestor: estimates can be inspected to observe the organism (or clade) that is adjacent to eukaryotes. Estimated phylogenies of ancient divergence events frequently suggest low uncertainty in their estimates as quantified through “bootstrap support” (the percentage of trees that support the split when estimation is performed on subsets of the sequence data) or posterior probability (the percentage of trees sampled from the posterior distribution that contain the split). However, it is common to see the complete absence of splits with bootstrap support and posterior probabilities exceeding 95% when the set of genes or genomes used for estimation are slightly modified (e.g., (Zhang et al. 2025, Figure 3c)). Estimates with more rigorous uncertainty quantification are clearly needed.

To illustrate how our estimation approach can be used to quantify the uncertainty in evolutionary divergence, we apply our method to study the divergence of eukaryotes from archaea. We focus in particular on Asgard archaea, which share more genes and gene similarity with eukaryotes than other archaeal clades; thus, the closest archaeal relative of Eukarya may fall in this group. Recently Zhang et al. (2025) reconstructed a large number of new Asgard archaeal genomes and combined them with existing data to investigate previous claims of

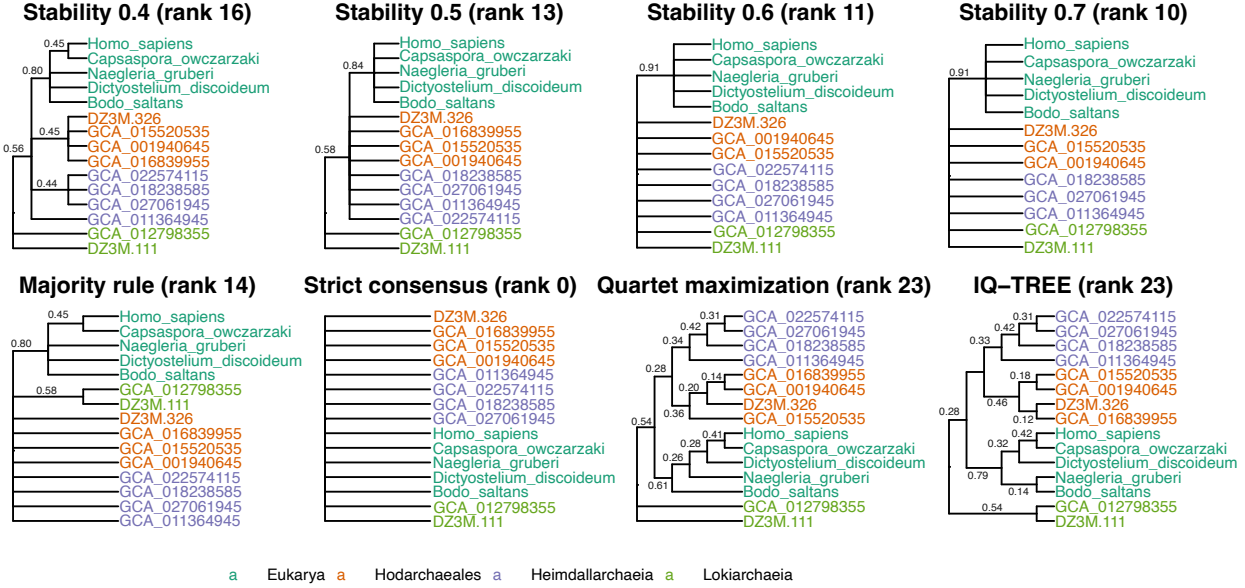


FIGURE 8. The phylogeny of genes shared between archaea and eukaryotes can be used to study the order of ancient evolution. We applied our method to random subsets of 85 multi-domain gene trees and estimated the α -stable trees for different values of α . We also show estimates from 3 existing consensus tree methods: majority rule, strict consensus, and quartet maximization. Finally, we show the maximum likelihood tree estimated using a concatenated alignment. All trees are unrooted and unweighted: splits are denoted by vertical branches, and horizontal branches without a vertical offset denote unresolved branches. Labels on internal edges indicate α -stability scores; leaf stability scores can be found in Table 1. Data from Zhang et al. (2025).

Eukarya evolving from within the Asgard class Heimdallarchaeia as a sister lineage to the order Hodarchaeales (Eme et al. 2023), as opposed to predating the diversification of the Asgard class Heimdallarchaeia. We focus specifically on the question of whether Eukaryotes branched from within or outside of Heimdallarchaeia.

We consider the S97 dataset of Zhang et al. (2025), which contains genes that were found in at least 60% of Asgard clade representatives. The S97 multiple sequence alignment (MSA) contained identified sequences from both archaeal and eukaryotic genomes; in addition, Zhang et al. (2025) published the individual markers for the archaeal genomes. Therefore, to identify the markers in the eukaryotic genes in the MSA, we trained sequence identification algorithms on the individual archaeal markers and applied them to the eukaryotic sequences in the MSA using (Eddy 2011, `hmmbuild` and `hmmsearch`, v3.4). For ease of interpretation, we focused on 15 organisms: 5 eukaryotes, 5 Hodarchaeales within the class Heimdallarchaeia, 3 Heimdallarchaeia that were not in the order Hodarchaeales, and 2 Lokiarchaeia (non-Heimdallarchaeia Asgard archaea). Representatives of these groups were chosen uniformly-at-random within these taxonomic ranks, excluding organisms whose names in the MSA could not be unambiguously matched to the supplementary taxonomy information. The eukaryotes were chosen deterministically as the 4 oldest eukaryotes within the 14 considered by Zhang et al. (2025), and *Homo sapiens*. After identifying and aligning these genes, we estimated the gene trees for these markers, omitting organisms for which no gene was detected (Wong et al. 2025, `iqtree3`, v3.0.1).

The final tree-valued dataset consists of $n = 85$ gene trees with between 6 and 15 leaves each (25%, 50% and 75% quantiles: 13, 14, 14), which we used to construct α -stable trees for $\alpha \in (0.4, 0.5, 0.6, 0.7)$. The overall leaf set \mathcal{X} thus has size $|\mathcal{X}| = 15$ leaves. In order to apply Algorithm 1 for this construction, the trees were unrooted and stripped of edge lengths, retaining only their topologies. The range of α values was chosen to provide a representative sampling of the interval $(0, 1)$ while avoiding overly strict concordance requirements, reflecting our expectation that the selected gene trees exhibit substantial topological discordance given the long . which we used to construct α -stable trees for $\alpha \in (0.4, 0.5, 0.6, 0.7)$. The overall leaf set \mathcal{X} thus has size

TABLE 1. Leaf stability scores for the data analysis considered in Section 7. Absent values indicate that the leaf was not sufficiently stable to be present on the tree.

Name	Quartet	IQ-TREE	Majority rule	$\alpha = 0.4$	$\alpha = 0.5$	$\alpha = 0.6$	$\alpha = 0.7$
<i>Bodo saltans</i>	0.71	0.67	0.76	0.76	0.79	0.78	0.78
<i>Capsaspora owczarzaki</i>	0.81	0.82	0.86	0.86	0.86	0.85	0.85
<i>Dictyostelium discoideum</i>	0.84	0.80	0.78	0.78	0.85	0.84	0.84
<i>Homo sapiens</i>	0.79	0.81	0.87	0.87	0.87	0.86	0.86
<i>Naegleria gruberi</i>	0.82	0.73	0.82	0.82	0.84	0.81	0.81
DZ3M.111	0.93	0.93	0.95	0.95	0.95	0.86	0.86
DZ3M.326	0.78	0.75	0.82	0.76	0.82	0.79	0.79
GCA_011364945	0.91	0.91	0.93	0.86	0.93	0.87	0.87
GCA_027061945	0.82	0.82	0.91	0.85	0.91	0.84	0.84
GCA_018238585	0.89	0.88	0.95	0.86	0.95	0.89	0.89
GCA_001940645	0.88	0.86	0.95	0.98	0.95	0.87	0.87
GCA_015520535	0.78	0.73	0.79	0.74	0.79	0.74	0.74
GCA_016839955	0.54	0.56	0.60	0.58	0.60	-	-
GCA_022574115	0.69	0.71	0.73	0.71	0.73	0.67	-
GCA_012798355	0.85	0.85	0.95	0.92	0.95	0.86	0.86

$|\mathcal{X}| = 15$ leaves. In order to apply Algorithm 1 for this construction, the trees were unrooted and stripped of edge lengths, retaining only their topologies. The range of α values was chosen to provide a representative sampling of the interval $(0, 1)$ while avoiding overly strict concordance requirements, reflecting our expectation that the selected gene trees exhibit substantial topological discordance given the evolutionary timescales under consideration.

The estimated trees are shown in Figure 8 along with α -stability values for each branch; α -stability values for the leaves can be found in Table 1. Trees corresponding to larger values of α have fewer features: the number of leaves on each tree is $(15, 15, 14, 13)$, and the number of splits on each tree is $(5, 2, 1, 1)$. This is to be expected, as the criterion for stability becomes more stringent as α increases. The estimates do not contain conflicting information, and differences can solely be attributed to adding or dropping leaves and edges. By definition, all feature stability values exceed the chosen value of α . Note that any alterations to the estimated tree can result in changes to a feature’s stability score (Equations (5) and (6)). This is the source of variability in the leaf stability scores shown in Table 1.

Even for the lowest value of α that we investigated, broad taxonomic groupings are recapitulated by the estimated trees, validating the estimation procedure. In particular, the presence of a branch separating eukaryotes and archaea at even the most stringent stability threshold ($\alpha = 0.7$) suggests good recovery of true positives. This branch is also present on the $\alpha = 0.8$ tree (not shown), though the leaf *Bodo saltans* is not present on this tree. For $\alpha \geq 0.85$, the α -stable tree is the set of unresolved trees T_0 (not shown). While it is surprising that very high thresholds for stability may preclude a domain-level split, this in part reflects the non-universality of the genes: only 70 out of 85 genes were present in *Bodo saltans*; only 73 were present in *Dictyostelium discoideum* and *Naegleria gruberi*; and only 75 were present in *Capsaspora owczarzaki* and *Homo sapiens*. However, this is not solely due to missing genes: the eukaryotes were monophyletic on only 66 of 77 trees with at least 2 eukaryotes, 66 of 76 trees with at least 3 eukaryotes, and 64 of 73 trees with at least 4 eukaryotes. This illustrates that even when taxa are missing from trees, our approach accounts for the complex interplay between the presence of leaves, the presence of branches, and the compatibility of branches. Additional validation for the recovery of true positives includes the presence of the branch separating *Capsaspora owczarzaki* and *Homo sapiens* from the remaining taxa when $\alpha \leq 0.4$: these eukaryotes are the only two opisthokonts in this taxon set, and are expected to branch together (Torruella et al. 2015).

We also compare our estimates with trees estimated using existing methods (Figure 8, lower panel), along with stability scores for the features estimated on these trees. Based on the 19 out of 85 trees that contain all leaves, we constructed majority rule and strict consensus estimates. The strict consensus tree did not resolve any branches, while the majority rule tree has 3 splits. With the exception of an additional split in the eukaryotes, majority rule tree coincides exactly with the 0.5-stable tree, despite that the 0.5-stable tree

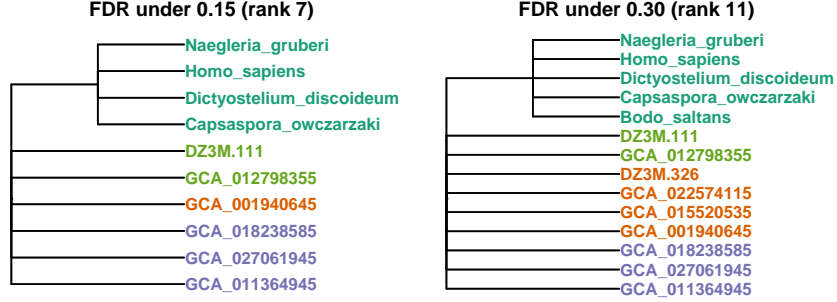


FIGURE 9. The phylogenetic trees built from 85 gene phylogenies shared across archaea and eukaryotes while controlling the false discovery rate at 15% and 30%. These estimates were obtained by first building an α -stable tree, then constructing a subposet, and finally building the trees by traversing the subposet.

did not require the restriction to trees with complete leaf sets. Indeed, our method does not require that any tree have a complete leaf set, and is therefore well-defined for a broader a set of inputs than majority rule. However, these methods differ also in their parameter space: α -stable trees may not contain the full leaf set \mathcal{X} .

We also show the quartet-maximizing tree as estimated using ASTRAL-III (v5.7.8) (Zhang et al. 2018), as well as the maximum likelihood tree estimated by Zhang et al. (2025) using IQ-TREE (v2.2.2.6) (Minh et al. 2020) applied to a concatenated alignment (we show the restriction to the 15 taxa under consideration). Both of these trees have the advantage of being estimated using the full tree dataset without the restriction to trees with complete leaf sets, but are fully resolved. While fully resolved trees provide more information on evolutionary relationships, the stability scores for splits estimated by ASTRAL-III and IQ-TREE range as low as 0.14 and 0.12, respectively. Therefore, even though these trees maximize their respective objective functions, low stability scores highlight weak evidence for many of the estimated relationships. We also note that there are multiple incongruities between these two fully resolved estimates: the branching within Hodarchaeales differs, and the branching within Eukarya differs.

We end this section by estimating early branching orders with FDR control, resulting in the trees shown in Figure 9. For this, we randomly sampled 45 of the 85 trees in the dataset to construct an α -stable tree with $\alpha = 0.4$. This stability threshold was selected to balance building a tree with consistent phylogenetic relationships while still obtaining a sufficiently complex subposet. Using this stable tree and the subsampled data, we constructed a subposet using Algorithm 3 with $\tau = 0.75$. Finally, we applied Algorithm 2 to the remaining 40 gene phylogenies and the subposet selecting $q \in \{0.10, 0.15, 0.20, 0.25, 0.30\}$. While the more stringent choice $q = 0.10$ yield no discoveries, $q = 0.15$ returned a tree containing a single branch separating eukaryotes from archaea, but only 10 of the original 15 organisms, including only 4 out of 5 eukaryotes. The overall rank of this tree is 7. For $q \in \{0.20, 0.25\}$, the estimated tree obtained from Algorithm 2 was unchanged relative to the tree estimated with $q = 0.15$. Finally, the $q = 0.3$ tree contains 14 organisms and a branch separating eukaryotes and archaea, for an overall rank of 11.

Taken together, these results demonstrate that there remains substantial uncertainty in the most recent archaeal ancestor of eukaryotic life. In contrast to existing methods, a key advantage of our approach is that it does not estimate a branching order when a split is uncertain. Instead, our approach may return a non-binary tree. Furthermore, it assigns stability scores to both edges and leaves, quantifying the evidence for a feature based on the collection of trees in the dataset. Finally, well-known and strongly supported relationships are resolved on our estimates, and the features present on the estimated trees are certainly true discoveries, even for low values of α .

8. DISCUSSION

Statistical procedures that control false discovery rates have been widely adopted in a variety of model selection problems because of their interpretable finite sample guarantees. In this paper, we applied this paradigm to the problem of estimating a summary tree from a tree-valued collection. In contrast to summary tree estimates

that optimize an objective function (e.g., quartet score, likelihood, or Fréchet loss), our approach sequentially builds the tree by evaluating whether the addition of a single feature (a leaf or an edge) is supported by the data. The resulting estimator collapses weakly supported structure and omits ambiguously placed leaves, yielding estimates that reflect discordance in the sample or uncertainty due to missingness. Our approach does not assume a fixed leaf set (unlike majority-rule thresholds) and does not force full resolution when the sample provides weak evidence (unlike most approaches to quartet maximization). To our knowledge, we provide the first FDR guarantee for tree estimation. In addition, our approach gives rise to an interpretable measure of uncertainty through stability scores, which provide a non-parametric assessment of the evidence for the features on any tree with respect to a collection of trees. In particular, stability scores can be used without applying our estimation procedure, and we use them to illustrate the low evidence in gene trees for quartet- and likelihood-maximizing consensus tree estimates in a data example.

Several future directions arise from our work, as outlined next.

Data generating distributions \mathcal{F} and population trees T^* satisfying Assumption 2. Our error rate guarantees are with respect to a data-independent tree T^* , defined implicitly by the data-generating distribution \mathcal{F} through Assumption 2. Recall from Remark 1 that this assumption can be modified so that the minimum probability of having no support for a null covering pair is at least η . Future work to characterize the set of T^* satisfying Assumption 2 (or its modified version) is warranted for important tree generative models such as Brownian motion on BHV tree space (Woodman & Nye 2025) and the multispecies coalescent model (Rannala & Yang 2003). Nonetheless, our simulations suggest that the species tree under the coalescent model satisfies the assumption for $\eta = 1/2$, and may even do so for larger values of η , which could account for why our procedure was conservative in simulations.

Designing more powerful procedures. There are several sources of conservatism to consider when seeking to make our procedure more powerful – i.e., to produce higher-complexity trees while still controlling the FDR. First, as described above, Assumption 2 may be satisfied for a larger value of η ; a larger value of η results in less stringent thresholds in our algorithm and thus a more powerful procedure. A second source of conservatism stems from our technical analysis in the proof of Lemma 10. Here, a minimum over a collection of covering pairs is upper bounded by a sum. A tighter analysis would again lead to less stringent thresholds. Third, sample splitting is required to ensure FDR control, as subposet construction and subposet traversal on the same data would constitute double-dipping. However the need to work with a subposet could be bypassed by having uniform convergence guarantees of $\frac{1}{|\mathcal{D}|} \sum_{T^{(\ell)} \in \mathcal{D}} \mathbb{I}[\rho(T_u, T^{(\ell)}) < \rho(T_v, T^{(\ell)})]$ to $\mathbb{P}[\rho(T_u, T^{(\ell)}) < \rho(T_v, T^{(\ell)})]$ simultaneously over all covering pairs (T_u, T_v) in the poset. This uniform convergence requires a characterization of the Rademacher complexity of the function class $\mathcal{G} = \{f_{u,v}(T) = \mathbb{I}[\rho(T_u, T) < \rho(T_v, T)] : (T_u, T_v) \text{ a covering pair}\}$.

Improving computational complexity. A key limitation of our method is its computational expense, precluding the analysis of trees with approximately 20 or more leaves on a modern laptop. A major bottleneck is the computation of the similarity function ρ , which involves identifying common splits between two trees (after removing incongruence-inducing leaves) and iteratively constructing the subset that yields the highest-rank tree. Some strategies could substantially accelerate this step. A stochastic greedy search could explore admissible edge subsets more efficiently, potentially reaching high-rank configurations without exhaustively evaluating low-cardinality subsets. Moreover, a more efficient internal representation of tree edges could further reduce the cost of the edge comparisons necessary for the computation of ρ .

Additional improvements may come from reducing redundancy in our implementation of Algorithm 1. In the current implementation, feature stabilities are recomputed each time a feature is added. However, it is feasible to characterize sufficient statistics for stability and to update them incrementally. For example, implementing data structures that group and order trees in the sample by their complexity and shared features may enable the exclusion of certain trees not-contributing to the score for the current candidate, thus avoiding unnecessary computation in evaluating ρ .

Weighting complexity. The notion of tree complexity in (1) views the addition of a split and the addition of a leaf as comparable forms of increasing complexity. However, it may be natural in some contexts to consider split additions as contributing more to the tree’s complexity than the inclusion of additional leaf. As such, we

can define a weighted notion of complexity:

$$\text{complexity}_\omega(T) := \begin{cases} |\mathcal{S}(T)| + \omega(|\mathcal{L}(T)| - 4) & T \notin T_0, \\ 0 & T \in T_0, \end{cases}$$

where $\omega > 0$. The parameter ω adjusts the relative contribution of leaf additions to the overall complexity score. When $\omega = 1$, this definition reduces exactly to the rank function in (1), treating splits and leaves as equally informative. For smaller values of ω , the complexity measure places greater emphasis on splits relative to leaves. Unlike the rank function, however, the weighted complexity does not take integer values when ω is non-integer. Still, it preserves the important property that larger trees in the poset have greater complexity values, provided $\omega > 0$. The case $\omega = 0$ is excluded, as it would ignore leaf additions entirely and break monotonicity with respect to the partial order. The weighted complexity measure yields a weighted notion of false discovery rate. Controlling this weighted error would require a new upper bound on the weighted false discovery proportion akin to the one in (8).

ACKNOWLEDGMENTS

Maria A Valdez Cabrera and Amy D Willis acknowledge funding from NSF 2415614 and NIH NIGMS R35 GM133420. Armeen Taeb acknowledges funding from NSF grant DMS-2413074.

REFERENCES

- Adams, III, E. N. (1972), ‘Consensus techniques and the comparison of taxonomic trees’, *Systematic Biology* **21**(4), 390–397.
- Allman, E. S., Degnan, J. H. & Rhodes, J. A. (2011), ‘Determining species tree topologies from clade probabilities under the coalescent.’, *Journal of Theoretical Biology* **289**, 96–106.
- Allman, E. S., Degnan, J. H. & Rhodes, J. A. (2016), ‘Species tree inference from gene splits by unrooted star methods’, *IEEE/ACM Transactions on Computational Biology and Bioinformatics* **15**, 337–342.
- Asnicar, F., Thomas, A., Beghini, F., Mengoni, C., Manara, S., Manghi, P., Zhu, Q., Bolzan, M., Cumbo, F., May, U., Sanders, J., Zolfo, M., Kopylova, E., Pasolli, E., Knight, R., Mirarab, S., Huttenhower, C. & Segata, N. (2020), ‘Precise phylogenetic analysis of microbial isolates and genomes from metagenomes using PhyloPhlAn 3.0’, *Nature Communications* **11**(1), 1–10.
- Avni, E. & Snir, S. (2018), ‘Reconstruction of real and simulated phylogenies based on quartet plurality inference’, *BMC Genomics* **19**(6), 19–29.
- Avni, E. & Snir, S. (2019), ‘A new quartet-based statistical method for comparing sets of gene trees is developed using a generalized hoeffding inequality’, *Journal of Computational Biology* **26**(1), 27–37.
- Barthélemy, J.-P. & McMorris, F. R. (1986), ‘The median procedure for n-trees’, *Journal of Classification* **3**(2), 329–334.
- Bendich, P., Marron, J. S., Miller, E., Pieloch, A. & Skwerer, S. (2016), ‘Persistent homology analysis of brain artery trees’, *The Annals of Applied Statistics* **10**(1), 198–218.
- Benjamini, Y. & Hochberg, Y. (1995), ‘Controlling the false discovery rate: a practical and powerful approach to multiple testing’, *Journal of the Royal Statistical Society: Series B* **57**, 289–300.
- Betts, H. C., Puttick, M. N., Clark, J. W., Williams, T. A., Donoghue, P. C. J. & Pisani, D. (2018), ‘Integrated genomic and fossil evidence illuminates life’s early evolution and eukaryote origin’, *Nature Ecology & Evolution* **2**(10), 1556–1562.
- Breiman, L. (2001), ‘Random Forests’, *Machine Learning* **45**(1), 5–32.
- Chernomor, O., Von Haeseler, A. & Minh, B. Q. (2016), ‘Terrace aware data structure for phylogenomic inference from supermatrices’, *Systematic Biology* **65**(6), 997–1008.
- Darwin, C. (1859), *On the Origin of Species by Means of Natural Selection, or the Preservation of Favoured Races in the Struggle for Life*, John Murray, London. First edition.
- Degnan, J. H., Degiorgio, M., Bryant, D. & Rosenberg, N. A. (2008), ‘Properties of consensus methods for inferring species trees from gene trees.’, *Systematic Biology* **58** **1**, 35–54.
- Degnan, J. H., DeGiorgio, M., Bryant, D. & Rosenberg, N. A. (2009), ‘Properties of consensus methods for inferring species trees from gene trees’, *Systematic Biology* **58**(1), 35–54.
- Degnan, J. H. & Rosenberg, N. A. (2009), ‘Gene tree discordance, phylogenetic inference and the multispecies coalescent.’, *Trends in Ecology & Evolution* **24**(6), 332–340.
- Eddy, S. R. (2011), ‘Accelerated profile HMM searches’, *PLOS Computational Biology* **7**(10), e1002195.

- Eme, L., Tamarit, D., Caceres, E. F., Stairs, C. W., De Anda, V., Schön, M. E., Seitz, K. W., Dombrowski, N., Lewis, W. H., Homa, F., Saw, J. H., Lombard, J., Nunoura, T., Li, W.-J., Hua, Z.-S., Chen, L.-X., Banfield, J. F., John, E. S., Reysenbach, A.-L., Stott, M. B., Schramm, A., Kjeldsen, K. U., Teske, A. P., Baker, B. J. & Ettema, T. J. G. (2023), ‘Inference and reconstruction of the Heimdallarchaeial ancestry of eukaryotes’, *Nature* **618**(7967), 992–999.
- Felsenstein, J. (1997), ‘An alternating least squares approach to inferring phylogenies from pairwise distances’, *Systematic Biology* **46**(1), 101–111.
- Felsenstein, J. (2004), *Inferring Phylogenies*, Sinauer Associates, Sunderland.
- Fogg, J., Allman, E. S. & Ané, C. (2023), ‘Phylocoalsimulations: a simulator for network multispecies coalescent models, including a new extension for the inheritance of gene flow’, *Systematic Biology* **72**(5), 1171–1179.
- Galtier, N. (2007), ‘A model of horizontal gene transfer and the bacterial phylogeny problem’, *Systematic Biology* **56**(4), 633–642.
- Gray, R. D. & Atkinson, Q. D. (2003), ‘Language-tree divergence times support the Anatolian theory of Indo-European origin’, *Nature* **426**(6965), 435–439.
- G’Sell, M. G., Wager, S., Chouldechova, A. & Tibshirani, R. (2013), ‘Sequential selection procedures and false discovery rate control’, *Journal of the Royal Statistical Society: Series B* **78**.
- Haydon, D. T., Chase-Topping, M., Shaw, D. J., Matthews, L., Friar, J. K., J Wilesmith & Woolhouse, M. E. J. (2003), ‘The construction and analysis of epidemic trees with reference to the 2001 UK foot-and-mouth outbreak.’, *Proceedings of the Royal Society B: Biological Sciences* **270**(1511), 121–127.
- Imachi, H., Nobu, M. K., Nakahara, N., Morono, Y., Ogawara, M., Takaki, Y., Takano, Y., Uematsu, K., Ikuta, T., Ito, M., Matsui, Y., Miyazaki, M., Murata, K., Saito, Y., Sakai, S., Song, C., Tasumi, E., Yamanaka, Y., Yamaguchi, T., Kamagata, Y., Tamaki, H. & Takai, K. (2020), ‘Isolation of an archaeon at the prokaryote–eukaryote interface’, *Nature* **577**(7791), 519–525.
- Larget, B. R., Kotha, S. K., Dewey, C. N. & Ané, C. (2010), ‘BUCKy: Gene tree/species tree reconciliation with Bayesian concordance analysis’, *Bioinformatics (Oxford, England)* **26**(22), 2910–2911.
- Lee, M. D. (2019), ‘GToTree: A user-friendly workflow for phylogenomics’, *Bioinformatics (Oxford, England)* **35**(20), 4162–4164.
- Legried, B., Molloy, E. K., Warnow, T. & Roch, S. (2021), ‘Polynomial-time statistical estimation of species trees under gene duplication and loss’, *Journal of Computational Biology: A Journal of Computational Molecular Cell Biology* **28**(5), 452–468.
- Li, A. & Barber, R. F. (2015), ‘Accumulation tests for FDR control in ordered hypothesis testing’, *Journal of the American Statistical Association* **112**, 837 – 849.
- Liu, L., Yu, L. & Edwards, S. V. (2010), ‘A maximum pseudo-likelihood approach for estimating species trees under the coalescent model’, *BMC Evolutionary Biology* **10**(302).
- Lynch, G., Guo, W., Sarkar, S. K. & Finner, H. (2016), ‘The control of the false discovery rate in fixed sequence multiple testing’, *Electronic Journal of Statistics* **11**, 4649–4673.
- Maddison, W. P. (1997), ‘Gene trees in species trees’, *Systematic Biology* **46**(3), 523–536.
- Margush, T. & McMorris, F. R. (1981), ‘Consensus n-trees’, *Bulletin of Mathematical Biology* **43**(2), 239–244.
- Markin, A. & Eulenstein, O. (2021), ‘Quartet-based inference is statistically consistent under the unified duplication-loss-coalescence model’, *Bioinformatics* **37**(22), 4064–4074.
- Miller, E., Owen, M. & Provan, J. S. (2015), ‘Polyhedral computational geometry for averaging metric phylogenetic trees’, *Advances in Applied Mathematics* **68**, 51–91.
- Minh, B. Q., Schmidt, H. A., Chernomor, O., Schrempf, D., Woodhams, M. D., von Haeseler, A. & Lanfear, R. (2020), ‘IQ-TREE 2: New models and efficient methods for phylogenetic inference in the genomic era’, *Molecular Biology and Evolution* **37**(5), 1530–1534.
- Mirarab, S., Reaz, R., Bayzid, M. S., Zimmermann, T., Swenson, M. S. & Warnow, T. J. (2014), ‘Astral: genome-scale coalescent-based species tree estimation’, *Bioinformatics* **30**, i541 – i548.
- Nakhleh, L., Warnow, T., Ringe, D. & Evans, S. N. (2005), ‘A comparison of phylogenetic reconstruction methods on an Indo-European dataset’, *Transactions of the Philological Society* **103**(2), 171–192.
- O’Reilly, J. E. & Donoghue, P. C. J. (2017), ‘The efficacy of consensus tree methods for summarizing phylogenetic relationships from a posterior sample of trees estimated from morphological data’, *Systematic Biology* **67**, 354 – 362.
- Pamilo, P. & Nei, M. (1988), ‘Relationships between gene trees and species trees.’, *Molecular Biology and Evolution* **5**(5), 568–583.

- Ramdas, A., Chen, J., Wainwright, M. & Jordan, M. (2019), ‘DAGGER: A sequential algorithm for FDR control on DAGs’, *Biometrika* **106**, 69–86.
- Rannala, B. & Yang, Z. (2003), ‘Bayes estimation of species divergence times and ancestral population sizes using dna sequences from multiple loci’, *Genetics* **164**(4), 1645–1656.
- Robinson, D. F. & Foulds, L. R. (1981), ‘Comparison of phylogenetic trees’, *Mathematical Biosciences* **53**(1), 131–147.
- Saitou, N. & Nei, M. (1987), ‘The neighbor-joining method: A new method for reconstructing phylogenetic trees.’, *Molecular Biology and Evolution* **4**(4), 406–425.
- Sayyari, E. & Mirarab, S. (2016), ‘Fast coalescent-based computation of local branch support from quartet frequencies’, *Molecular Biology and Evolution* **33**(7), 1654–1668.
- Segata, N., Börnigen, D., Morgan, X. C. & Huttenhower, C. (2013), ‘PhyloPhlAn is a new method for improved phylogenetic and taxonomic placement of microbes’, *Nature Communications* **4**(1), 1–11.
- Szöllősi, G. J., Rosikiewicz, W., Boussau, B., Tannier, E. & Daubin, V. (2013), ‘Efficient exploration of the space of reconciled gene trees’, *Systematic Biology* **62**(6), 901–912.
- Taeb, A., Bühlmann, P. & Chandrasekaran, V. (2024), ‘Model selection over partially ordered sets’, *Proceedings of the National Academy of Sciences of the United States of America* **121**.
- Than, C. V. & Rosenberg, N. A. (2011), ‘Consistency properties of species tree inference by minimizing deep coalescences’, *Journal of Computational Biology* **18** **1**, 1–15.
- Torruella, G., de Mendoza, A., Grau-Bové, X., Antó, M., Chaplin, M. A., del Campo, J., Eme, L., Pérez-Cordón, G., Whipps, C. M., Nichols, K. M., Paley, R., Roger, A. J., Sitjà-Bobadilla, A., Donachie, S. & Ruiz-Trillo, I. (2015), ‘Phylogenomics reveals convergent evolution of lifestyles in close relatives of animals and fungi’, *Current Biology* **25**(18), 2404–2410.
- Wang, H. & Marron, J. S. (2007), ‘Object oriented data analysis: Sets of trees’, *The Annals of Statistics* **35**(5), 1849–1873.
- Wong, T., Ly-Trong, N., Ren, H., Baños, H., Roger, A., Susko, E., Bielow, C., De Maio, N., Goldman, N., Hahn, M., Huttley, G., Lanfear, R. & Minh, B. Q. (2025), ‘IQ-TREE 3: Phylogenomic inference software using complex evolutionary models’.
- Woodman, W. M. & Nye, T. M. (2025), ‘Brownian motion, bridges and bayesian inference in phylogenetic tree space’, *arXiv preprint arXiv:2506.22135*.
- Wu, M. & Eisen, J. A. (2008), ‘A simple, fast, and accurate method of phylogenomic inference’, *Genome Biology* **9**(10), R151.
- Yan, Z., Smith, M. L., Du, P., Hahn, M. W. & Nakhleh, L. (2022), ‘Species tree inference methods intended to deal with incomplete lineage sorting are robust to the presence of paralogs’, *Systematic Biology* **71**(2), 367–381.
- Yekutieli, D. (2008), ‘Hierarchical false discovery rate-controlling methodology’, *Journal of the American Statistical Association* **103**, 309–316.
- Zhang, C., Rabiee, M., Sayyari, E. & Mirarab, S. (2018), ‘ASTRAL-III: Polynomial time species tree reconstruction from partially resolved gene trees’, *BMC Bioinformatics* **19**(6), 153.
- Zhang, J., Feng, X., Li, M., Liu, Y., Liu, M., Hou, L.-J. & Dong, H.-P. (2025), ‘Deep origin of eukaryotes outside Heimdallarchaeia within Asgardarchaeota’, *Nature* pp. 1–9.

APPENDIX

APPENDIX A. PROOFS

A.1. Proof of Theorem 1.

Proof. In particular, reflexivity ($T \preceq T$) straightforwardly holds. To show anti-symmetry ($T_1 \preceq T_2$ and $T_2 \preceq T_1$ implies $T_1 = T_2$), the first condition of ordering relationship implies that the leaf sets are identical, and the second condition of ordering allows us to conclude that the split sets are identical. This allows us to conclude that $T_1 = T_2$. To show transitivity ($T_1 \preceq T_2$ and $T_2 \preceq T_3$ implies $T_1 \preceq T_3$), we have $\mathcal{L}(T_1) \subseteq \mathcal{L}(T_2)$, $\mathcal{L}(T_2) \subseteq \mathcal{L}(T_3)$ and that $\mathcal{S}(T_1) \subseteq \Phi_{\mathcal{L}(T_1)}(\mathcal{S}(T_2))$, $\mathcal{S}(T_2) \subseteq \Phi_{\mathcal{L}(T_2)}(\mathcal{S}(T_3))$. Note that:

$$\mathcal{S}(T_1) \subseteq \Phi_{\mathcal{L}(T_1)}(\mathcal{S}(T_2)) \subseteq \Phi_{\mathcal{L}(T_1)}(\mathcal{S}(\Phi_{\mathcal{L}(T_2)}(T_3))) = \Phi_{\mathcal{L}(T_1)}\Phi_{\mathcal{L}(T_2)}(\mathcal{S}(T_3)) = \Phi_{\mathcal{L}(T_1)}(\mathcal{S}(T_3)).$$

Here, we have used the fact that the map Φ and \mathcal{S} commute, and that $\Phi_{\mathcal{L}(T_1)}\Phi_{\mathcal{L}(T_2)}(\cdot) = \Phi_{\mathcal{L}(T_1)}(\cdot)$ since $\mathcal{L}(T_1) \subseteq \mathcal{L}(T_2)$. Furthermore, $\mathcal{L}(T_1) \subseteq \mathcal{L}(T_3)$. Thus, $T_1 \preceq T_3$. \square

A.2. Proof of Theorem 2.

Proof. Suppose that $T_1 \preceq T_2$ with $\text{rank}(T_1) + 1 < \text{rank}(T_2)$. We prove that there must exist a distinct tree T such that $T_1 \preceq T \preceq T_2$. We consider three cases:

(Case 1) $\mathcal{L}(T_2) = \mathcal{L}(T_1)$: In this case $\Phi_{\mathcal{L}(T_1)}(\mathcal{S}(T_2)) = \mathcal{S}(T_2)$, and since $|\mathcal{L}(T_1)| = |\mathcal{L}(T_2)|$, then the condition $\text{rank}(T_1) + 1 < \text{rank}(T_2)$ implies there is at least two internal edges $s_1, s_2 \in \mathcal{S}(T_2) \setminus \mathcal{S}(T_1)$. Consider the tree T with $\mathcal{L}(T) = \mathcal{L}(T_1)$ and $\mathcal{S}(T) = \mathcal{S}(T_1) \cup s_1$. Then we can readily verify $T \neq T_1, T_2$ and $T_1 \preceq T \preceq T_2$.

(Case 2) $\mathcal{L}(T_2) = \mathcal{L}(T_1) \cup \{\ell\}$: In this case $|\mathcal{L}(T_2)| = |\mathcal{L}(T_1)| + 1$ and the condition $\text{rank}(T_1) + 1 < \text{rank}(T_2)$ implies $|\mathcal{S}(T_2)| \geq |\mathcal{S}(T_1)| + 1$. There are two options: $\mathcal{S}(T_1) = \Phi_{\mathcal{L}(T_1)}(\mathcal{S}(T_2))$ or $\mathcal{S}(T_1) \subset \Phi_{\mathcal{L}(T_1)}(\mathcal{S}(T_2))$.

For the first option, this would imply there are two internal edges $s_1, s_2 \in \mathcal{S}(T_2)$ that satisfy $\Phi_{\mathcal{L}(T_1)}(s_1) = \Phi_{\mathcal{L}(T_1)}(s_2)$. If we take T such that $\mathcal{L}(T) = \mathcal{L}(T_2)$ and $\mathcal{S}(T) = \mathcal{S}(T_2) \setminus \{s_2\}$ we obtain a tree such that $T \neq T_1, T_2$ and $T_1 \preceq T \preceq T_2$. For the second option, we take T to be the tree with $\mathcal{L}(T) = \mathcal{L}(T_1)$ and $\mathcal{S}(T) = \Phi_{\mathcal{L}(T_1)}(\mathcal{S}(T_2))$, which also results in $T_1 \preceq T \preceq T_2$.

(Case 3) $|\mathcal{L}(T_2)| > |\mathcal{L}(T_1)| + 1$: Take one of the leaves in T_2 that are not in T_1 , $\ell \in \mathcal{L}(T_2) \setminus \mathcal{L}(T_1)$. If we take $T = \Phi_{\mathcal{L}(T_1) \cup \{\ell\}}(T_2)$, then $T_1 \preceq T \preceq T_2$. \square

A.3. Proof of Lemma 4.

Proof. Suppose there exists a maximal common tree $\tilde{T} \in \mathcal{M}(T, T^{(\ell)})$ where $a \notin \mathcal{L}(\tilde{T})$. By definition, $\tilde{T} \preceq T$. Recall that $T_{\downarrow \text{leaf } a}$ is a tree with leaf set $\mathcal{S}(T) \setminus \{a\}$ and split set $\Phi_{\mathcal{S}(T) \setminus \{a\}}(\mathcal{S}(T))$. Since $a \notin \mathcal{L}(\tilde{T})$, we have that:

$$\mathcal{S}(\tilde{T}) \subseteq \Phi_{\mathcal{L}(\tilde{T})}(\mathcal{S}(T)) = \Phi_{\mathcal{L}(\tilde{T})}\Phi_{\mathcal{L}(T) \setminus \{a\}}(\mathcal{S}(T)) = \Phi_{\mathcal{L}(\tilde{T})}(\mathcal{S}(T_{\downarrow \text{leaf } a})),$$

where we have used $\Phi_{\mathcal{L}(\tilde{T})}\Phi_{\mathcal{L}(T) \setminus \{a\}}(\cdot) = \Phi_{\mathcal{L}(\tilde{T})}(\cdot)$ since $\mathcal{L}(\tilde{T}) \subseteq \mathcal{L}(T) \setminus \{a\}$. Thus, we conclude that $\tilde{T} \preceq T_{\downarrow \text{leaf } a}$. By monotonicity property of similarity function, we have:

$$\rho(T_{\downarrow \text{leaf } a}, T^{(\ell)}) = \max_{\substack{\tilde{T} \preceq T_{\downarrow \text{leaf } a} \\ \tilde{T} \preceq T^{(\ell)}}} \text{rank}(\tilde{T}) \leq \max_{\substack{\tilde{T} \preceq T \\ \tilde{T} \preceq T^{(\ell)}}} \text{rank}(\tilde{T}) = \rho(T, T^{(\ell)})$$

Since a maximizer \tilde{T} on the right-hand-side of the inequality is also a feasible tree in the optimization problem on the left-hand-side of the inequality (i.e., $\tilde{T} \preceq T_{\downarrow \text{leaf } a}$), we conclude that: $\rho(T_{\downarrow \text{leaf } a}, T^{(\ell)}) = \rho(T, T^{(\ell)})$.

Now, suppose $a \in \mathcal{L}(\tilde{T})$ for all $\tilde{T} \in \mathcal{M}(T, T^{(\ell)})$. Suppose as a point of contradiction that $\rho(T_{\downarrow \text{leaf } a}, T^{(\ell)}) = \rho(T, T^{(\ell)})$. Take $\tilde{T} \in \mathcal{M}(T_{\downarrow \text{leaf } a}, T^{(\ell)})$. Since \tilde{T} must satisfy $\tilde{T} \preceq T_{\downarrow \text{leaf } a}$, then $a \notin \mathcal{L}(\tilde{T})$. Since $T_{\downarrow \text{leaf } a}$, by transitivity property of posets, we have $\tilde{T} \preceq T$. Since, additionally, $\text{rank}(\tilde{T}) = \text{rank}(T)$, this means that $\tilde{T} \in \mathcal{M}(T, T^{(\ell)})$. We reach a contradiction since a maximal common subtree \tilde{T} does not have leaf a . \square

A.4. Proof of Lemma 7.

Proof. \Leftarrow : $(T_a, T_b) \in \mathcal{C}_{\text{null}}$ implies that $\text{FD}(T_a, T^*) < \text{FD}(T_b, T^*)$. Indeed, by assumption we have $\rho(T_a, T^*) = \rho(T_b, T^*)$. Combining this with the facts that $\text{FD}(T_a, T^*) = \text{rank}(T_a) - \rho(T_a, T^*)$, $\text{FD}(T_b, T^*) = \text{rank}(T_b) - \rho(T_b, T^*)$, and $\text{rank}(T_b) = \text{rank}(T_a) + 1$, we have that $\text{FD}(T_a, T^*) < \text{FD}(T_b, T^*)$.

\Rightarrow : $\text{FD}(T_a, T^*) < \text{FD}(T_b, T^*)$ implies that $(T_a, T_b) \in \mathcal{C}_{\text{null}}$. Suppose as contradiction that $(T_a, T_b) \notin \mathcal{C}_{\text{null}}$. By the monotonicity property of similarity function, this means that $\rho(T_a, T^*) < \rho(T_b, T^*)$. Since the similarity function measures the rank of a maximal common subtree, and the rank function takes non-negative integer values, $\rho(T_a, T^*) < \rho(T_b, T^*)$ implies that $\rho(T_b, T^*) - \rho(T_a, T^*) \geq 1$. Combining this with the facts that $\text{FD}(T_a, T^*) = \text{rank}(T_a) - \rho(T_a, T^*)$, $\text{FD}(T_b, T^*) = \text{rank}(T_b) - \rho(T_b, T^*)$, and $\text{rank}(T_b) = \text{rank}(T_a) + 1$, we reach a contradiction. \square

A.5. Proof of Lemma 5.

Proof. First assume there exist a tree $\tilde{T} \in \mathcal{M}(T, T^{(\ell)})$ for which $\Phi_{\mathcal{L}(\tilde{T})}(A|B) \notin \mathcal{S}(\tilde{T})$. Since $\tilde{T} \preceq T$, then for every $\tilde{e} \in E(\tilde{T})$ there is an edge $e_1 \in E(T) \setminus \{e\} = E(T_{\downarrow \text{edge } e})$ for which $\Phi_{\mathcal{L}(\tilde{T})}(S_{e_1}) = S_{\tilde{e}}$. Thus, $\tilde{T} \preceq T_{\downarrow \text{edge } e}$ and $\rho(T_{\downarrow \text{edge } e}, T^{(\ell)}) = \rho(T, T^{(\ell)})$. Which means $\rho(T_{\downarrow \text{edge } e}, T^{(\ell)}) < \rho(T, T^{(\ell)})$ implies that for all $\tilde{T} \in \mathcal{M}(T, T^{(\ell)})$, there exists $e' \in E(\tilde{T})$ such that $\Phi_{\mathcal{L}(\tilde{T})}(A|B) = S_{e'}$.

Now assume for a tree $\tilde{T} \in \mathcal{M}(T, T^{(\ell)})$, there exists $e' \in E(\tilde{T})$ such that $\Phi_{\mathcal{L}(\tilde{T})}(A|B) = S_{e'}$, but there exists a leaf subset $L \in U_T(e)$ associated with the adjacent edge e^* to e for which $L \cap \mathcal{L}(\tilde{T}) = \emptyset$. Since any $x \in \mathcal{L}(\tilde{T})$ is such that $x \notin A^* \triangle A$, then $A \cap \mathcal{L}(\tilde{T}) = A^* \cap \mathcal{L}(\tilde{T})$. This implies $\Phi_{\mathcal{L}(\tilde{T})}(S_e) = \Phi_{\mathcal{L}(\tilde{T})}(S_{e^*})$, which would imply $\tilde{T} \preceq T_{\downarrow \text{edge } e}$.

This establishes $\rho(T_{\downarrow \text{edge } e}, T^{(\ell)}) < \rho(T, T^{(\ell)}) \Rightarrow$ for all $\tilde{T} \in \mathcal{M}(T, T^{(\ell)})$, there exists $e' \in E(\tilde{T})$ such that $\Phi_{\mathcal{L}(\tilde{T})}(S_e) = S_{e'}$, and for all leaf-subsets $\mathcal{L}' \in U_T(e)$ there exists $a_{\mathcal{L}'} \in \mathcal{L}'$ such that $a_{\mathcal{L}'} \in \mathcal{L}(\tilde{T})$.

If $\rho(T_{\downarrow \text{edge } e}, T^{(\ell)}) = \rho(T, T^{(\ell)})$, then there exists $\tilde{T} \in \mathcal{M}(T, T^{(\ell)})$ such that $\tilde{T} \preceq T_{\downarrow \text{edge } e}$. If there exists $e' \in E(\tilde{T})$ such that $\Phi_{\mathcal{L}(\tilde{T})}(S_e) = S_{e'}$, then $\tilde{T} \preceq T_{\downarrow \text{edge } e}$ implies another edge $e_1 \in E(T) \setminus \{e\}$ is such that $\Phi_{\mathcal{L}(\tilde{T})}(S_{e_1}) = S_{e'}$. Take $S_{e_1} = A_1|B_1$ with either $A_1 \subset A$ or $A \subset A_1$. This implies $A_1 \cap \mathcal{L}(\tilde{T}) = A \cap \mathcal{L}(\tilde{T})$, which implies $(A \triangle A_1) \cap \mathcal{L}(\tilde{T}) = \emptyset$.

Take $S_{e^*} = A^*|B^*$ the split associated to the adjacent edge to e between e_1 and e . By properties of splits in trees, if $A_1 \subset A$ then $A_1 \subset A^* \subset A$, and if $A_1 \supset A$ then $A_1 \supset A^* \supset A$. This implies $A^* \triangle A \subset A_1 \triangle A$. Thus, $(A \triangle A^*) \cap \mathcal{L}(\tilde{T}) = \emptyset$.

This establishes that if for all $\tilde{T} \in \mathcal{M}(T, T^{(\ell)})$, there exists $e' \in E(\tilde{T})$ such that $\Phi_{\mathcal{L}(\tilde{T})}(S_e) = S_{e'}$, and for all leaf-subsets $\mathcal{L}' \in U_T(e)$ there exists $a_{\mathcal{L}'} \in \mathcal{L}'$ such that $a_{\mathcal{L}'} \in \mathcal{L}(\tilde{T})$, then $\rho(T_{\downarrow \text{edge } e}, T^{(\ell)}) < \rho(T, T^{(\ell)})$. \square

A.6. Proof of Theorem 8.

The proof relies on the following lemmas.

Lemma 9. Consider any T such that for every covering pair (T_a, T_b) in \mathcal{P}_{sub} with $T_b \preceq T$, $\text{score}_{\mathcal{D}_2}(T_a, T_b) \geq \gamma(T_b, q)$. Let $(T_0, T_1, \dots, T_k := T)$ specify any path from T_0 to T in the poset \mathcal{P}_{sub} . Then:

$$\text{FDP}(T, T^*) \leq \frac{r_{\max} - \text{rank}(T_{j^*}) + 1}{r_{\max}} \mathbb{I}[\text{score}_{\mathcal{D}_2}(T_{j^*-1}, T_{j^*}) \geq \gamma(T_{j^*}, q)],$$

where $j^* = \text{argmin}\{j : \rho(T_{j-1}, T^*) = \rho(T_j, T^*)\}$.

Proof of Lemma 9. Note that $\text{FDP}(T, T^*) = \text{FD}(T, T^*)/\text{rank}(T)$. Additionally, define:

$$\begin{aligned} V &= \sum_i \mathbb{I}(\rho(T_{i-1}, T^*) = \rho(T_i, T^*)), \\ S &= \sum_i \mathbb{I}(\rho(T_{i-1}, T^*) < \rho(T_i, T^*)). \end{aligned}$$

Note that: $V + S = \text{rank}(T)$ and by the bound in (8), we have $\text{FD}(T, T^*) \leq V$. Thus,

$$\text{FDP}(T, T^*) = \text{FD}(T, T^*)/\text{rank}(T) \leq \frac{V}{V+S} = \frac{V}{V+S} \mathbb{I}(V > 0).$$

Since $\frac{V}{V+S}$ is an increasing function of V , the fact that $V \leq r_{\max} - \text{rank}(T_{j^*}) + 1$, and the sequential nature of our algorithm, we have that:

$$\begin{aligned} \text{FDP}(T, T^*) &\leq \frac{r_{\max} - \text{rank}(T_{j^*}) + 1}{r_{\max} - \text{rank}(T_{j^*}) + 1 + S} \mathbb{I}[\text{score}_{\mathcal{D}_2}(T_{j^*-1}, T_{j^*}) \geq \gamma(T_{j^*}, q)], \\ &\leq \frac{r_{\max} - \text{rank}(T_{j^*}) + 1}{r_{\max}} \mathbb{I}[\text{score}_{\mathcal{D}_2}(T_{j^*-1}, T_{j^*}) \geq \gamma(T_{j^*}, q)]. \end{aligned}$$

The last argument follows from $S \geq \text{rank}(T_{j^*}) - 1$. \square

Lemma 10. Consider any $T_M \in \mathcal{M}$. Let \mathcal{L} be a collection of covering pairs (T_a, T_b) such that $T_b \preceq T_M$, and no other pair (T'_a, T'_b) satisfies $T'_b \preceq T_a$. Then,

$$\sum_{(T_a, T_b) \in \mathcal{L}} \frac{1}{\kappa(T_b)} \leq \frac{1}{|\mathcal{M}|}.$$

Proof of Lemma 10. For simplicity, when we say a tree covers another one, we mean in the poset \mathcal{P}_{sub} . For every $h = 1, 2, \dots, \text{rank}(T_M)$, define $\mathcal{L}_h := \{(T_a, T_b) \in \mathcal{L} : \text{rank}(T_b) = h\}$. Let r be the smallest non-integer value such that \mathcal{L}_r is non-empty. Thus, we wish to bound:

$$\sum_{h=r}^{\text{rank}(T_M)} \sum_{(T_a, T_b) \in \mathcal{L}_h} \frac{1}{\kappa(T_b)}.$$

We first bound $\sum_{(T_a, T_b) \in \mathcal{L}_r} \frac{1}{\kappa(T_b)}$. Define

$$\mathcal{F}_{r+1} = \{\text{covering pair } (T_b, T'_b) \notin \mathcal{L}_{r+1} : (T_a, T_b) \in \mathcal{L}_r \text{ for some } T_a\}.$$

By the choice of the κ function, we have for any T' that covers T_b : $\kappa(T_b) \geq \kappa(T')(\# \text{ trees } T_b \text{ covers})$. Thus,

$$\begin{aligned} \sum_{(T_a, T_b) \in \mathcal{L}_r} \frac{1}{\kappa(T_b)} &\leq \sum_{(T_a, T_b) \in \mathcal{L}_r} \min_{\substack{T'_b: T'_b \text{ covers } T_b \\ (T_b, T'_b) \notin \mathcal{L}_{r+1}}} \frac{1}{\kappa(T'_b)(\# \text{ trees } T_b \text{ covers})}, \\ &\leq \sum_{(T_a, T_b) \in \mathcal{L}_r} \sum_{\substack{T'_b: T'_b \text{ covers } T_b \\ (T_b, T'_b) \notin \mathcal{L}_{r+1}}} \frac{1}{\kappa(T'_b)(\# \text{ trees } T_b \text{ covers})}, \\ &= \sum_{(T_b, T'_b) \in \mathcal{F}_{r+1}} \sum_{T_a: (T_a, T_b) \in \mathcal{L}_r} \frac{1}{\kappa(T'_b)(\# \text{ trees } T_b \text{ covers})} \\ &\leq \sum_{(T_b, T'_b) \in \mathcal{F}_{r+1}} \frac{1}{\kappa(T'_b)}. \end{aligned}$$

Our goal is next to bound: $\sum_{(T_a, T_b) \in \mathcal{F}_{r+1} \cup \mathcal{L}_{r+1}} \frac{1}{\kappa(T_b)}$. Define:

$$\mathcal{F}_{r+2} := \{\text{covering pair } (T_b, T'_b) \notin \mathcal{L}_{r+2} : (T_a, T_b) \in \mathcal{L}_{r+1} \cup \mathcal{F}_{r+1} \text{ for some } T_a\}.$$

We then have that:

$$\begin{aligned}
\sum_{(T_a, T_b) \in \mathcal{L}_{r+1} \cup \mathcal{F}_{r+1}} \frac{1}{\kappa(T_b)} &\leq \sum_{(T_a, T_b) \in \mathcal{L}_{r+1} \cup \mathcal{F}_{r+1}} \min_{\substack{T'_b: T'_b \text{ covers } T_b \\ (T_b, T'_b) \notin \mathcal{L}_{r+2}}} \frac{1}{\kappa(T'_b)(\# \text{ trees } T_b \text{ covers})}, \\
&\leq \sum_{(T_a, T_b) \in \mathcal{L}_{r+1} \cup \mathcal{F}_{r+1}} \sum_{\substack{T'_b: T'_b \text{ covers } T_b \\ (T_b, T'_b) \notin \mathcal{L}_{r+2}}} \frac{1}{\kappa(T'_b)(\# \text{ trees } T_b \text{ covers})}, \\
&\leq \sum_{(T_b, T'_b) \in \mathcal{F}_{r+2}} \frac{1}{\kappa(T'_b)}.
\end{aligned}$$

We repeatedly continue this argument until we obtain:

$$\sum_{h=r}^{\text{rank}(T_M)} \sum_{(T_a, T_b) \in \mathcal{L}_h} \frac{1}{\kappa(T_b)} = \sum_{(T_a, T_b) \in \mathcal{L}_{\text{rank}(T_M)} \cup \mathcal{F}_{\text{rank}(T_M)}} \frac{1}{\kappa(T_b)}.$$

By construction, $\mathcal{F}_{\text{rank}(T_M)} \cup \mathcal{L}_{\text{rank}(T_M)} = \{(T_a, T_M) : T_M \text{ covers } T_a\}$. Thus:

$$\sum_{h=r}^{\text{rank}(T_M)} \sum_{(T_a, T_b) \in \mathcal{L}_h} \frac{1}{\kappa(T_b)} = \sum_{(T_a, T_M) \text{ covering pair}} \frac{1}{\kappa(T_M)} = \frac{1}{|\mathcal{M}|}.$$

□

Proof of Theorem 8. Let O consist of a collection of trees T such that for every covering pair (T_a, T_b) in \mathcal{P}_{sub} with $T_b \preceq T'$, $\text{score}_{\mathcal{D}_2}(T_a, T_b) \geq \gamma(T_b, q)$. Since the output $\hat{T} \in O$, we have:

$$\text{FDP}(\hat{T}, T^*) \leq \max_{T \in O} \text{FDP}(T, T^*).$$

Fix a tree $T \in O$. Define the set:

$$\mathcal{F}(T) := \{(T_a, T_b) \text{ null covering pair} : T_b \preceq T; \text{ no null covering pair } (T'_a, T'_b) \text{ with } T'_b \preceq T_a\}.$$

By construction, for any $(T_a, T_b) \in \mathcal{F}(T)$, there exists a path from T_0 to T that traverses through (T_a, T_b) where this covering pair is the ‘first null covering pair’. From Lemma 9, we have:

$$\text{FDP}(T, T^*) \leq \frac{r_{\max} - \text{rank}(T_b) + 1}{r_{\max}} \mathbb{I}(\text{score}_{\mathcal{D}_2}(T_a, T_b) \geq \gamma(T_b, q)).$$

Define

$$\mathcal{H} := \{(T_a, T_b) \text{ null covering pair} : \text{ no null covering pair } (T'_a, T'_b) \text{ with } T'_b \preceq T_a\}.$$

By construction, $\mathcal{H} = \cup_{T \in \mathcal{T}_{\text{sub}}} \mathcal{F}(T)$. Then

$$\begin{aligned}
\text{FDP}(\hat{T}, T^*) &\leq \max_{T \in O} \left\{ \frac{r_{\max} - \text{rank}(T_b) + 1}{r_{\max}} \mathbb{I}[\text{score}_{\mathcal{D}_2}(T_a, T_b) \geq \gamma(T_b, q)] : (T_a, T_b) \in \mathcal{F}(T) \right\}, \\
&= \max \left\{ \frac{r_{\max} - \text{rank}(T_b) + 1}{r_{\max}} \mathbb{I}[\text{score}_{\mathcal{D}_2}(T_a, T_b) \geq \gamma(T_b, q)] : (T_a, T_b) \in \mathcal{H} \right\}, \\
&\leq \sum_{(T_a, T_b) \in \mathcal{H}} \frac{r_{\max} - \text{rank}(T_b) + 1}{r_{\max}} \mathbb{I}[\text{score}_{\mathcal{D}_2}(T_a, T_b) \geq \gamma(T_b, q)].
\end{aligned}$$

Combining everything and appealing to Hoeffding’s inequality, we have:

$$\mathbb{E}[\text{FDP}(\hat{T}, T^*)] \leq \sum_{(T_a, T_b) \in \mathcal{H}} \frac{r_{\max} - \text{rank}(T_b) + 1}{r_{\max}} \exp \left\{ -n_2 (\gamma(T_b, q) - 1/2)^2 \right\} = \sum_{(T_a, T_b) \in \mathcal{H}} \frac{q}{\kappa(T_b)}.$$

Appealing to Lemma 10, we have:

$$\mathbb{E}[\text{FDP}(\hat{T}, T^*)] \leq \sum_{T_M \in \mathcal{M}} \sum_{(T_a, T_b) \in \mathcal{H}(T_M)} \frac{q}{\kappa(T_b)} \leq \sum_{T_M \in \mathcal{M}} \frac{q}{|\mathcal{M}|} = q.$$

□

APPENDIX B. ALGORITHM TO COMPUTE ρ

Computing similarity. To quantify the similarity between two trees T_1 and T_2 , we construct a set of common splits – partitions of the leaf set that can be simultaneously supported by edges of both trees. For every pair consisting of one edge from T_1 and one edge from T_2 , we remove incongruent leaves until the two edges define the same partition on the remaining leaves, and this is recorded as a common split along with its set of leaves. Given any subset S of the common splits, it is possible to reconstruct a tree by retaining only the leaves in the intersection of the leaf sets across all splits. The edges of the reconstructed tree correspond precisely to the partitions defined by the splits in S , restricted to this common leaf set.

The similarity value $\rho(T_1, T_2)$ is equal to the maximum rank among all trees that can be assembled from such subsets. Beginning with an individual split, we incrementally construct potential subsets of common splits by adding additional splits whenever doing so does not reduce the common leaf set below a threshold required to exceed the current best rank. At each extension step, the rank of the induced tree is computed, and the global maximum is updated.

The search proceeds recursively over all feasible subsets, while discarding any edge for which no subset including it can yield a rank greater than or equal to the current maximum. This is determined based on an upper bound given by the number of leaves and the maximum number of edges that can still be added. The algorithm terminates once all subsets capable of generating a higher-ranked tree have been explored. The final similarity score ρ is the highest rank obtained through this process.

We implemented a depth-first search over subsets of common splits, using stacks to manage the current path and discard edges that cannot improve the current maximum rank. This implementation is detailed in Algorithm 4.

Algorithm 4 Computing tree similarity $\rho(T_1, T_2)$

```

1: Input: Trees  $T_1, T_2$ 
2: Compute the set of common splits  $S = \text{commonSplits}(T_1, T_2)$  ordered by number of leaves (decreasing)
3: Initialize  $\text{cur\_maxRank} \leftarrow$  rank of tree built with first split in  $S$ 
4: Initialize stacks:  $\text{indxC}$  (indices of splits),  $\text{curTrees}$  (current trees),  $\text{curRankPotential}$  (rank potential)
5: Set  $\text{Beginning} \leftarrow 0$ ,  $\text{End} \leftarrow |S|$ 
6: while  $\text{Beginning} < \text{End}$  do
7:   if  $\text{indxC}$  is empty then
8:     Push  $\text{Beginning}$  onto  $\text{indxC}$  stacks and initialize  $\text{curTrees}$  with corresponding partial tree
9:     Push its rank potential to  $\text{curRankPotential}$ 
10:  end if
11:  Let  $i = \text{indxC.top}()$ 
12:  if rank potential of  $i \leq \text{cur\_maxRank}$  then
13:    Pop  $\text{indxC}$ ,  $\text{curTrees}$ ,  $\text{curRankPotential}$ 
14:    Update  $\text{End}$  to  $i$ 
15:  else
16:    if  $i + 1 < \text{End}$  then
17:      Push  $i + 1$  onto  $\text{indxC}$ 
18:      Extend partial tree with split  $S[i + 1]$  and update rank potential of the new tree
19:      if new tree rank  $> \text{cur\_maxRank}$  then
20:         $\text{cur\_maxRank} \leftarrow$  new tree rank
21:      end if
22:    else
23:      Pop  $\text{indxC}$ ,  $\text{curTrees}$ ,  $\text{curRankPotential}$ 
24:    end if
25:  end if
26:  if  $\text{indxC}$  is empty then
27:     $\text{Beginning} \leftarrow i + 1$ 
28:    if Potential rank with edges between  $\text{Beginning}$  and  $\text{End} \leq \text{cur\_maxRank}$  then
29:      break
30:    end if
31:  end if
32: end while
33: return  $\text{cur\_maxRank}$ 

```
